Journal of Algebra ••• (••••) •••–•••

Contents lists available at ScienceDirect

Journal of Algebra

journal homepage: www.elsevier.com/locate/jalgebra

Promotion and growth diagrams for fans of Dyck paths and vacillating tableaux

Joseph Pappe [a], Stephan Pfannerer [b,*], Anne Schilling [a,*], Mary Claire Simone [a]

[a] *Department of Mathematics, University of California, One Shields Avenue, Davis, CA 95616-8633, USA*
[b] *Institut für Diskrete Mathematik und Geometrie, TU Wien, Austria*

ARTICLE INFO

Article history:
Received 3 February 2023
Available online xxxx
Communicated by Alberto Elduque

Dedicated to Georgia Benkart

MSC:
05E10
05A19
05E18
15A72

Keywords:
Crystal bases
Virtual crystals
Promotion
Fomin growth diagrams
Dyck paths
Chord diagrams

ABSTRACT

We construct an injection from the set of r-fans of Dyck paths (resp. vacillating tableaux) of length n into the set of chord diagrams on $[n]$ that intertwines promotion and rotation. This is done in two different ways, namely as fillings of promotion matrices and in terms of Fomin growth diagrams. Our analysis uses the fact that r-fans of Dyck paths and vacillating tableaux can be viewed as highest weight elements of weight zero in crystals of type B_r and C_r, respectively, which in turn can be analyzed using virtual crystals. On the level of Fomin growth diagrams, the virtualization process corresponds to the Roby–Krattenthaler blow up construction. One of the motivations for finding rotation invariant diagrammatic bases such as chord diagrams is the cyclic sieving phenomenon. Indeed, we give a cyclic sieving phenomenon on r-fans of Dyck paths and vacillating tableaux using the promotion action.

* Corresponding authors.
E-mail addresses: jhpappe@ucdavis.edu (J. Pappe), stephan.pfannerer@tuwien.ac.at (S. Pfannerer), anne@math.ucdavis.edu (A. Schilling), mcsimone@ucdavis.edu (M.C. Simone).
URL: http://www.math.ucdavis.edu/~anne (A. Schilling).

https://doi.org/10.1016/j.jalgebra.2023.07.038

1. Introduction

Interest in invariant subspaces goes back to Rumer, Teller and Weyl [34], who studied the quantum mechanical description of molecules. In particular, they devised diagrammatic bases for the invariant spaces. For SL(n), a set of diagrams spanning the invariant space was constructed by Cautis, Kamnitzer and Morrison [5], generalizing Kuperberg's webs [22] for SL(2) and SL(3).

The dimension of the invariant subspace of a tensor product $V^{\otimes N}$ of an irreducible representation V of a Lie algebra $\mathfrak{g}$ is equal to the number of highest weight elements of weight zero in $\mathcal{B}^{\otimes N}$, where $\mathcal{B}$ is the crystal basis associated to V [43,30]. The symmetric group acts on $V^{\otimes N}$ by permuting tensor positions. By Schur–Weyl duality, this action commutes with the action of the Lie group. In particular, the symmetric group acts on the invariant space of $V^{\otimes N}$. It was shown by Westbury [43] that the action of the long cycle corresponds to the action of promotion on highest weight elements of weight zero in $\mathcal{B}^{\otimes N}$. In this setting promotion is defined using Henriques' and Kamnitzer's commutor [12], see [7,43,44]. Note that the full action of the symmetric group on invariant tensors is not yet known in general.

In general, it is desirable to have a correspondence between highest weight elements of weight zero in $\mathcal{B}^{\otimes N}$ and diagram bases, such as chord diagrams, which intertwine promotion and rotation. For Kuperberg's webs [22], this was achieved by Petersen, Pylyavskyy and Rhoades [29], Russell [35] and Patrias [28] by showing that the growth algorithm of Khovanov and Kuperberg [19] intertwines promotion with rotation. For the vector representation of the symplectic group and the adjoint representation of the general linear group, such a correspondence between highest weight elements of weight zero and chord diagrams which intertwines promotion and rotation was given in [30].

In this paper, we construct an injection from the set of r-fans of Dyck paths (resp. vacillating tableaux) of length n into the set of chord diagrams on $[n]$ that intertwines promotion and rotation. There is a natural correspondence between r-fans of Dyck paths (resp. vacillating tableaux) and highest weight elements in the tensor product of the spin crystal (resp. vector representation) of type B_r. We present this injection in two different ways:

(1) as fillings of promotion matrices [23] (see Section 3.1);
(2) in terms of Fomin growth diagrams [9,32,21] (see Sections 3.2-3.4).

While the first description shows that the map intertwines promotion and rotation, the second description shows injectivity. Our proof strategy uses virtualization of crystals (see for example [3]) and results of [30] for oscillating tableaux of weight zero (or equivalently highest weight words of weight zero for the vector representation type C_r):

Please cite this article in press as: J. Pappe et al., Promotion and growth diagrams for fans of Dyck paths and vacillating tableaux, J. Algebra (2023), https://doi.org/10.1016/j.jalgebra.2023.07.038

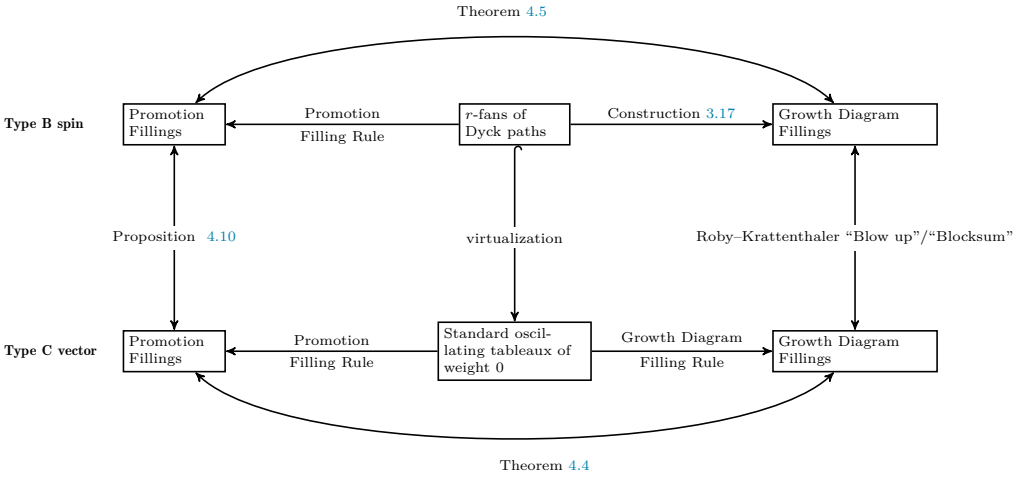

Fig. 1. Overview of strategy and results for r-fans of Dyck paths.

(1) Find a virtual crystal morphism for the spin crystals (resp. crystals for the vector representation) of type B_r into the r-th (resp. second) tensor power of the crystal of the vector representation of type C_r (see Section 2.2).
(2) Use this virtualization to map an r-fan of Dyck paths (resp. vacillating tableau) to an oscillating tableau (see Section 2.3).
(3) Show that this virtualization commutes with promotion and the filling rules.
(4) Show that blowing up the filling of the growth diagram corresponds to the filling of the oscillating tableau. In this sense, the blow up on growth diagrams is the analogue of the virtualization on crystals.

An overview of our strategy is shown in Figs. 1 and 2.

Having the injective map to chord diagrams gives a first step towards a diagrammatic basis for the invariant subspaces. In addition, Fontaine and Kamnitzer [7] as well as Westbury [43] tied the promotion action on highest weight elements of weight zero to the cyclic sieving phenomenon introduced by Reiner, Stanton and White [33]. In Section 4.4, we make this cyclic sieving phenomenon more concrete by providing the polynomial in terms of the energy function. For r-fans of Dyck paths, we conjecture another polynomial, which is the q-deformation of the number of r-fans of Dyck paths, to give a cyclic sieving phenomenon. For vacillating tableaux, we give a polynomial inspired by work of Jagenteufel [16] for a cyclic sieving phenomenon.

The paper is organized as follows. In Section 2, we give a brief review of crystal bases and virtual crystals and provide the virtual crystals for spin and vector representation of type B_r into type C_r. We also define promotion on crystals via the crystal commutor. In Section 3, we give the various filling rules to construct the map to chord diagrams. Section 4 is reserved for the statements and proofs of our main results.

Please cite this article in press as: J. Pappe et al., Promotion and growth diagrams for fans of Dyck paths and vacillating tableaux, J. Algebra (2023), https://doi.org/10.1016/j.jalgebra.2023.07.038

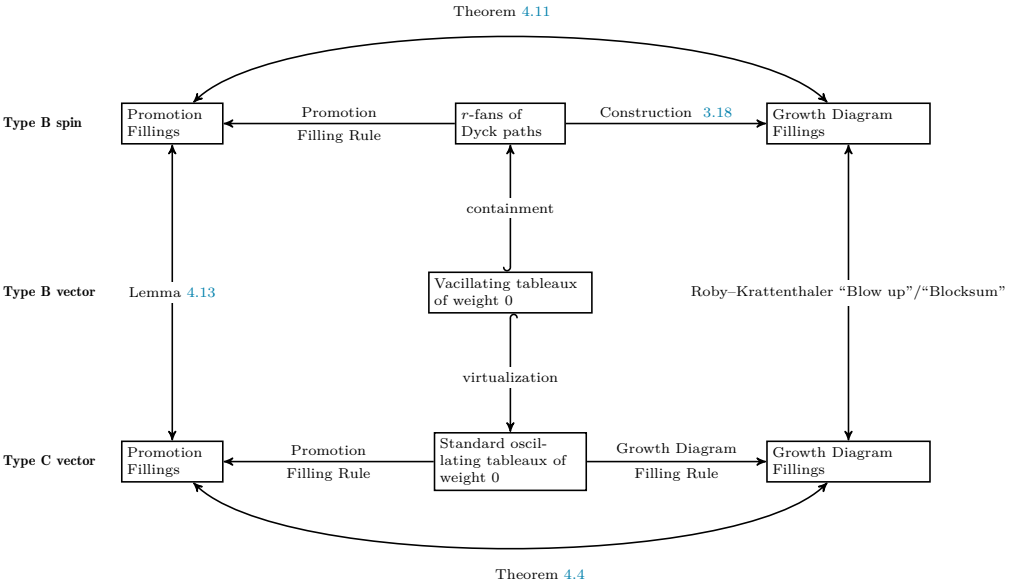

Fig. 2. Overview of strategy and results for vacillating tableaux.

Acknowledgments

We wish to thank Sam Hopkins, Joel Kamnitzer, Christian Krattenthaler, Vic Reiner, Martin Rubey, Travis Scrimshaw and Bruce Westbury for discussions. We especially thank Bruce Westbury for his communications regarding Theorem 4.22.

SP was the recipient of a DOC Fellowship of the Austrian Academy of Sciences. AS was partially supported by NSF grants DMS–1760329 and DMS–2053350.

2. Crystal bases

2.1. Background on crystals

Crystal bases form a combinatorial skeleton of representations of quantum groups associated to Lie algebras. They were first introduced by Kashiwara [17] and Lusztig [24].

Axiomatically, for a given root system Φ with index set I and weight lattice Λ, a *crystal* is a nonempty set $\mathcal{B}$ together with maps

$$\begin{aligned} e_i, f_i &\colon \mathcal{B} \to \mathcal{B} \sqcup \{\emptyset\} \\ \varepsilon_i, \varphi_i &\colon \mathcal{B} \to \mathbb{Z} \\ \mathsf{wt} &\colon \mathcal{B} \to \Lambda \end{aligned} \tag{2.1}$$

for $i \in I$, satisfying certain conditions (see for example [3, Definition 2.13]). The operators e_i and f_i are called *raising* and *lowering operators*. The map wt is the *weight map*. The

map ε_i (resp. φ_i) measures how often e_i (resp. f_i) can be applied to the given crystal element. For all crystals considered in this paper, we have for $b \in \mathcal{B}$

$$\varepsilon_i(b) = \max\{k \geqslant 0 \mid e_i^k(b) \neq \emptyset\} \quad \text{and} \quad \varphi_i(b) = \max\{k \geqslant 0 \mid f_i^k(b) \neq \emptyset\}. \tag{2.2}$$

An element $b \in \mathcal{B}$ is called *highest weight* if $e_i(b) = \emptyset$ for all $i \in I$.

Here we define certain crystals for the root systems B_r and C_r explicitly. Let $\mathbf{e}_i \in \mathbb{Z}^r$ be the i-th unit vector with 1 in position i and 0 everywhere else.

Definition 2.1. The *spin crystal* of type B_r, denoted by $\mathcal{B}_{\mathsf{spin}}$, consists of all r-tuples $\epsilon = (\epsilon_1, \epsilon_2, \ldots, \epsilon_r)$, where $\epsilon_i \in \{\pm\}$. The weight of ϵ is

$$\mathsf{wt}(\epsilon) = \frac{1}{2}\sum_{i=1}^{r} \epsilon_i \mathbf{e}_i.$$

The crystal operator f_r annihilates ϵ unless $\epsilon_r = +$. If $\epsilon_r = +$, f_r acts on ϵ by changing ϵ_r from $+$ to $-$ and leaving all other entries unchanged. The crystal operator f_i for $1 \leqslant i < r$ annihilates ϵ unless $\epsilon_i = +$ and $\epsilon_{i+1} = -$. In the latter case, f_i acts on ϵ by changing ϵ_i to $-$ and ϵ_{i+1} to $+$. Similarly, the crystal operator e_r annihilates ϵ unless $\epsilon_r = -$. If $\epsilon_r = -$, e_r acts on ϵ by changing ϵ_r from $-$ to $+$. The crystal operator e_i for $1 \leqslant i < r$ annihilates ϵ unless $\epsilon_i = -$ and $\epsilon_{i+1} = +$. In the latter case, e_i acts on ϵ by changing ϵ_i to $+$ and ϵ_{i+1} to $-$.

The crystal $\mathcal{B}_{\mathsf{spin}}$ of type B_3 is depicted in Fig. 3.

Definition 2.2. Here we define the *crystals for the vector representation* of type B_r and C_r.

(1) The crystal $\mathcal{C}_\square$ of type C_r consists of the elements $\{1, 2, \ldots, r, \overline{r}, \ldots, \overline{2}, \overline{1}\}$. The crystal operator f_i for $1 \leqslant i < r$ maps i to $i+1$, maps $\overline{i+1}$ to $\overline{i}$ and annihilates all other elements. The crystal operator f_r maps r to $\overline{r}$ and annihilates all other elements. Similarly, the crystal operator e_i for $1 \leqslant i < r$ maps $i+1$ to i, maps $\overline{i}$ to $\overline{i+1}$ and annihilates all other elements. The crystal operator e_r maps $\overline{r}$ to r and annihilates all other elements. Furthermore, $\mathsf{wt}(i) = \mathbf{e}_i$ and $\mathsf{wt}(\overline{i}) = -\mathbf{e}_i$.

(2) The crystal $\mathcal{B}_\square$ of type B_r consists of the elements $\{1, 2, \ldots, r, 0, \overline{r}, \ldots, \overline{2}, \overline{1}\}$. The crystal operator f_i for $1 \leqslant i < r$ maps i to $i+1$, maps $\overline{i+1}$ to $\overline{i}$ and annihilates all other elements. The crystal operator f_r maps r to 0, 0 to $\overline{r}$ and annihilates all other elements. Similarly, the crystal operator e_i for $1 \leqslant i < r$ maps $i+1$ to i, maps $\overline{i}$ to $\overline{i+1}$ and annihilates all other elements. The crystal operator e_r maps $\overline{r}$ to 0, 0 to r and annihilates all other elements. Furthermore, $\mathsf{wt}(i) = \mathbf{e}_i$ and $\mathsf{wt}(\overline{i}) = -\mathbf{e}_i$ for $i \neq 0$ and $\mathsf{wt}(0) = 0$.

The crystals $\mathcal{C}_\square$ for type C_2 and $\mathcal{B}_\square$ for type B_2 are depicted in Fig. 4.

Please cite this article in press as: J. Pappe et al., Promotion and growth diagrams for fans of Dyck paths and vacillating tableaux, J. Algebra (2023), https://doi.org/10.1016/j.jalgebra.2023.07.038

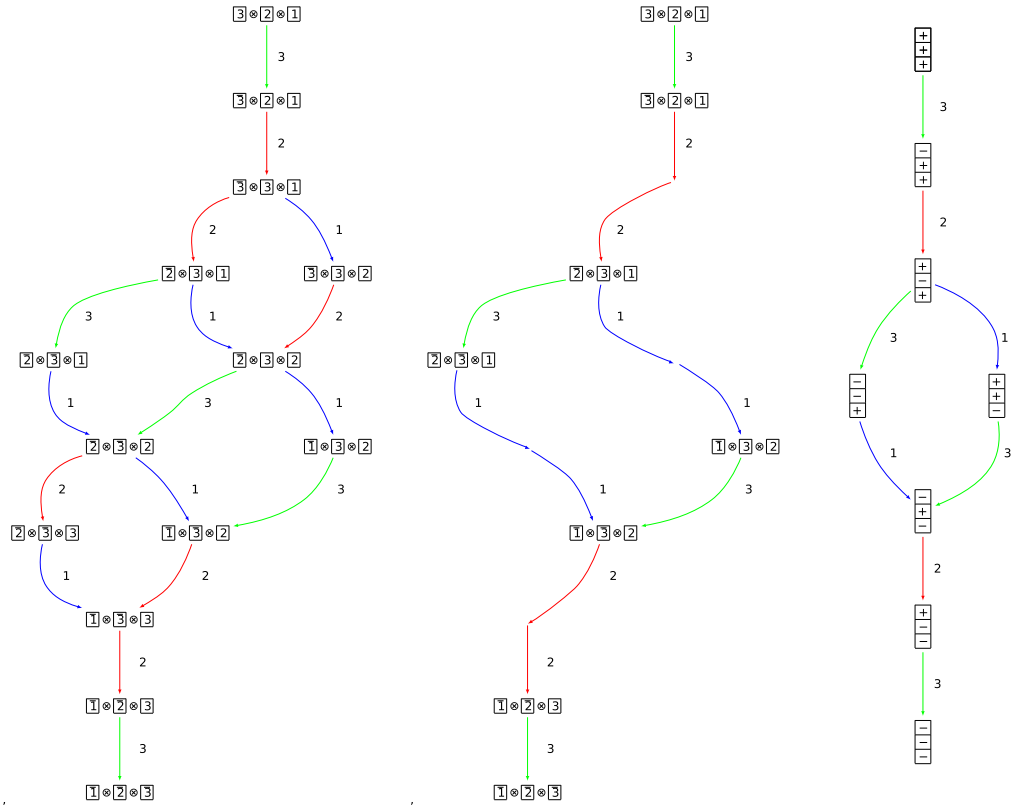

Fig. 3. Left: One component of the crystal $\widehat{\mathcal{V}} = \mathcal{C}_{\square}^{\otimes 3}$ of type C_3. Middle: The virtual crystal $\mathcal{V}$ inside $\widehat{\mathcal{V}}$ of type B_3. Right: The spin crystal $\mathcal{B}_{\mathsf{spin}}$ of type B_3.

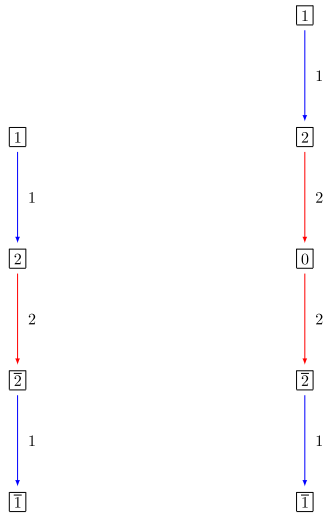

Fig. 4. Left: The crystal $\mathcal{C}_{\square}$ of type C_2. Right: The crystal $\mathcal{B}_{\square}$ of type B_2.

Please cite this article in press as: J. Pappe et al., Promotion and growth diagrams for fans of Dyck paths and vacillating tableaux, J. Algebra (2023), https://doi.org/10.1016/j.jalgebra.2023.07.038

A remarkable property of crystals is that they respect *tensor products*. Given two crystals $\mathcal{B}$ and $\mathcal{C}$ associated to the same root system Φ, the tensor product $\mathcal{B} \otimes \mathcal{C}$ as a set is the Cartesian product $\mathcal{B} \times \mathcal{C}$. The weight of $b \otimes c \in \mathcal{B} \otimes \mathcal{C}$ is the sum of the weights $\mathsf{wt}(b \otimes c) = \mathsf{wt}(b) + \mathsf{wt}(c)$. Furthermore

$$f_i(b \otimes c) = \begin{cases} f_i(b) \otimes c & \text{if } \varphi_i(c) \leqslant \varepsilon_i(b), \\ b \otimes f_i(c) & \text{if } \varphi_i(c) > \varepsilon_i(b), \end{cases}$$

and

$$e_i(b \otimes c) = \begin{cases} e_i(b) \otimes c & \text{if } \varphi_i(c) < \varepsilon_i(b), \\ b \otimes e_i(c) & \text{if } \varphi_i(c) \geqslant \varepsilon_i(b). \end{cases}$$

2.2. Virtual crystals

Stembridge [39] characterized crystals which are associated with quantum group representations for simply-laced root systems in terms of local rules on the crystal graph. Crystals for non-simply-laced root systems can be constructed using virtual crystals, see [3, Chapter 5].

In this paper, we utilize virtual crystals to construct Fomin growth diagrams and the promotion operators for type B_r using results for type C_r. Hence let us briefly review the set-up for virtual crystals. Let $X \hookrightarrow Y$ be an embedding of Lie algebras such that the fundamental weights ω_i and simple roots α_i map as follows

$$\omega_i^X \mapsto \gamma_i \sum_{j \in \sigma(i)} \omega_j^Y,$$
$$\alpha_i^X \mapsto \gamma_i \sum_{j \in \sigma(i)} \alpha_j^Y.$$

Here γ_i is a multiplication factor, $\sigma \colon I^X \to I^Y / \operatorname{aut}$ is a bijection and aut is an automorphism on the Dynkin diagram for Y.

Let $\widehat{\mathcal{V}}$ be an ambient crystal associated to the Lie algebra Y. In [3, Chapter 5] it is assumed that $\widehat{\mathcal{V}}$ is a crystal for a simply-laced root system. However, in general it may be assumed that $\widehat{\mathcal{V}}$ is a crystal corresponding to a quantum group representation (which is the case in our setting).

Definition 2.3. If there is an embedding of Lie algebras $X \hookrightarrow Y$, then $\mathcal{V} \subseteq \widehat{\mathcal{V}}$ is a *virtual crystal* for the root system Φ^X if

V1. The ambient crystal $\widehat{\mathcal{V}}$ is a Stembridge crystal or a crystal associated to a representation for the root system Φ^Y with crystal operators $\widehat{e}_i$, $\widehat{f}_i$, $\widehat{\varepsilon}_i$, $\widehat{\varphi}_i$ for $i \in I^Y$ and weight function $\widehat{\mathsf{wt}}$.

Please cite this article in press as: J. Pappe et al., Promotion and growth diagrams for fans of Dyck paths and vacillating tableaux, J. Algebra (2023), https://doi.org/10.1016/j.jalgebra.2023.07.038

V2. If $b \in \mathcal{V}$ and $i \in I^X$, then $\widehat{\varepsilon}_j(b)$ has the same value for all $j \in \sigma(i)$ and that value is a multiple of γ_i. The same is true for $\widehat{\varphi}_j(b)$.

V3. The subset $\mathcal{V} \sqcup \{\emptyset\} \subseteq \widehat{\mathcal{V}} \sqcup \{\emptyset\}$ is closed under the virtual crystal operators

$$e_i := \prod_{j \in \sigma(i)} \widehat{e}_j^{\gamma_i} \quad \text{and} \quad f_i := \prod_{j \in \sigma(i)} \widehat{f}_j^{\gamma_i}.$$

Furthermore, for all $b \in \mathcal{V}$

$$\varepsilon_i(b) = \max\{k \geqslant 0 \mid e_i^k(b) \neq \emptyset\} \quad \text{and} \quad \varphi_i(b) = \max\{k \geqslant 0 \mid f_i^k(b) \neq \emptyset\}.$$

The tensor product of two virtual crystals for the same embedding $X \hookrightarrow Y$ is again a virtual crystal (see for example [3, Theorem 5.8]).

2.2.1. Virtual crystal $B_r \hookrightarrow C_r$ spin to vector

We will now apply the theory of virtual crystals to the embedding $B_r \hookrightarrow C_r$. In this setting $I^{C_r} = I^{B_r} = \{1, 2, \ldots, r\}$, $\sigma(i) = \{i\}$, $\gamma_i = 2$ for $1 \leqslant i < r$ and $\gamma_r = 1$. We consider as the ambient crystal

$$\widehat{\mathcal{V}} = \mathcal{C}_{\square}^{\otimes r}.$$

Define an ordering $<$ on the set $[r] \cup [\bar{r}]$ as follows:

$$1 < 2 < \cdots < r < \bar{r} < \cdots < \bar{1}.$$

Denote by $|\cdot|$ the map from $[r] \cup [\bar{r}]$ to $[r]$ that sends letters to their corresponding unbarred values.

Definition 2.4. Let $\mathcal{V} \subseteq \widehat{\mathcal{V}}$ be given by

$$\mathcal{V} := \{v_r \otimes v_{r-1} \otimes \cdots \otimes v_1 \in \widehat{\mathcal{V}} \mid v_i > v_j \text{ and } |v_i| \neq |v_j| \text{ for all } i > j\}.$$

Let $f_i = \widehat{f}_i^2$, $e_i = \widehat{e}_i^2$ for $1 \leqslant i < r$ and $f_r = \widehat{f}_r$, $e_r = \widehat{e}_r$.

Lemma 2.5. *$\mathcal{V} \sqcup \{\emptyset\}$ is closed under the operators f_i and e_i for $1 \leqslant i \leqslant r$.*

Proof. Let $v = v_r \otimes v_{r-1} \otimes \cdots \otimes v_1 \in \mathcal{V}$. We break into cases depending on the value of i.

Assume that $i = r$. By the definition of $\mathcal{V}$, v must either contain an r or $\bar{r}$, but not both. If v contains an r, then this r must be to the left of all other unbarred letters and to the right of all barred letters. As f_r changes the r to a $\bar{r}$, $f_r(v)$ is still in $\mathcal{V}$. If v contains an $\bar{r}$, then $f_r(v) = \emptyset \in \mathcal{V} \sqcup \{\emptyset\}$.

Assume that $i \neq r$. Note that the conditions imposed on v imply that there exists exactly two indices j and k such that $|v_j| = i$ and $|v_k| = i + 1$. By the ordering imposed on v, v can only be in the following forms:

- $\cdots \otimes i+1 \otimes i \otimes \cdots$
- $\cdots \otimes \bar{i} \otimes \overline{i+1} \otimes \cdots$
- $\cdots \otimes \bar{i} \otimes \cdots \otimes i+1 \otimes \cdots$
- $\cdots \otimes \overline{i+1} \otimes \cdots \otimes i \otimes \cdots$

For the first three cases, $f_i(v) = \emptyset$. When v is of the form $\cdots \otimes \overline{i+1} \otimes \cdots \otimes i \otimes \cdots$, f_i replaces the $\overline{i+1}$ with $\bar{i}$ and the i with $i+1$. Since v does not contain an $\bar{i}$ nor an $i+1$, $f_i(v)$ is an element of $\mathcal{V}$.

The fact that $e_i(v) \in \mathcal{V}$ for all $i \in 1 \leqslant i \leqslant r$ follows similarly. Thus, $\mathcal{V}$ is closed under the operators f_i and e_i. □

Lemma 2.6. *All elements of $\mathcal{V}$ are in the connected component of $\widehat{\mathcal{V}}$ with highest weight element $r \otimes r-1 \otimes \cdots \otimes 1$.*

Proof. Clearly $r \otimes r-1 \otimes \cdots \otimes 1$ is a highest weight element of $\widehat{\mathcal{V}}$ and the only element in $\mathcal{V}$ without any barred letters.

Consider $v = v_r \otimes \cdots \otimes v_1 \in \mathcal{V}$ containing a barred letter. Observe that the number of barred letters in $e_i(v)$ is at most the number of barred letters in v whenever $e_i(v) \neq \emptyset$. Since $\widehat{\mathcal{V}}$ is finite and $\mathcal{V}$ is closed under e_i, it suffices to show that $e_i(v) \neq \emptyset$ for some i. Let v_j denote the rightmost tensor factor in v that is a barred letter, and let $i = |v_j|$. We break into cases depending on the value of i.

If $i = r$, then $v_j = \bar{r}$ and v cannot contain an r. This implies that $e_r(v) \neq \emptyset$ as it acts on v by replacing v_j by r. The number of barred letters has decreased by one.

If $i \neq r$, then $v_j = \bar{i}$. As v_j is the rightmost barred letter in v, v must be of the form $\cdots \otimes \bar{i} \otimes \cdots \otimes i+1 \otimes \cdots$. Thus, e_i acts by changing $\bar{i}$ to $\overline{i+1}$ and $i+1$ to i. Note that the rightmost barred letter is closer to $\bar{r}$. □

Definition 2.7. Let $\Psi \colon \mathcal{B}_{\mathsf{spin}} \to \mathcal{V}$ be the map

$$\Psi(\epsilon_1 \epsilon_2 \cdots \epsilon_r) = v_r \otimes v_{r-1} \otimes \cdots \otimes v_1,$$

where $v_r > v_{r-1} > \cdots > v_1$ such that if $\epsilon_i = +$ then v contains an i and if $\epsilon_i = -$ then v contains an $\bar{i}$ for all $1 \leqslant i \leqslant r$.

Lemma 2.8. *The map Ψ is a bijective map that intertwines the crystal operators on $\mathcal{B}_{\mathsf{spin}}$ and $\mathcal{V}$.*

Proof. From the definition of Ψ, it is clearly bijective. Let $\epsilon = \epsilon_1 \epsilon_2 \cdots \epsilon_r \in \mathcal{B}_{\mathsf{spin}}$. Since the raising and lowering operators of a crystal are partial inverses, it suffices to prove that $f_i(\epsilon) \neq \emptyset$ if and only if $f_i(\Psi(\epsilon)) \neq \emptyset$ and $\Psi(f_i(\epsilon)) = f_i(\Psi(\epsilon))$ whenever $f_i(\epsilon) \neq \emptyset$.

Assume that $f_i(\Psi(\epsilon)) \neq \emptyset$. If $i = r$, then $\Psi(\epsilon)$ contains an r implying $\epsilon_r = +$. Therefore $f_r(\epsilon) \neq \emptyset$. If $i \neq r$, then ϵ contains both an i and an $\overline{i+1}$. Thus, $\epsilon_i = +$ and $\epsilon_{i+1} = -$ implying $f_i(\epsilon) \neq \emptyset$.

Please cite this article in press as: J. Pappe et al., Promotion and growth diagrams for fans of Dyck paths and vacillating tableaux, J. Algebra (2023), https://doi.org/10.1016/j.jalgebra.2023.07.038

Assume that $f_i(\epsilon) \neq \emptyset$. If $i = r$, then $\epsilon_r = +$ and f_r acts on ϵ by replacing ϵ_r with a $-$. This implies that $\Psi(f_r(\epsilon))$ can be obtained from $\Psi(\epsilon)$ by changing the r to $\bar{r}$, which agrees with the action of f_r. Therefore $\Psi(f_r(\epsilon)) = f_r(\Psi(\epsilon))$. If $i \neq r$, then ϵ_i must be a $+$ and ϵ_{i+1} must be a $-$. Thus, f_i swaps the signs of ϵ_i and ϵ_{i+1}. Since $\epsilon_i = +$ and $\epsilon_{i+1} = -$, $\Psi(\epsilon)$ must contain both an $\overline{i+1}$ and an i. This implies $\Psi(f_i(\epsilon))$ can be obtained from $\Psi(\epsilon)$ by replacing the $\overline{i+1}$ with $\bar{i}$ and the i with $i+1$. Observe that f_i acts on $\Psi(\epsilon)$ in exactly the same manner. Hence, $\Psi(f_i(\epsilon)) = f_i(\Psi(\epsilon))$. □

Proposition 2.9. *$\mathcal{V}$ is a virtual crystal for the embedding of Lie algebras $B_r \hookrightarrow C_r$.*

Proof. The ambient crystal $\widehat{\mathcal{V}}$ is a crystal coming from a representation (see for example [3]), ensuring **V1**. Using Lemmas 2.5 and 2.8, we have $\Psi(\mathcal{B}_{\mathsf{spin}}) = \mathcal{V}$ is closed under the crystal operators f_i and e_i. Since the elements in both $\mathcal{B}_{\mathsf{spin}}$ and $\widehat{\mathcal{V}}$ satisfy (2.2), the string lengths of $\mathcal{B}_{\mathsf{spin}}$ are the same as the string lengths in $\mathcal{V}$, showing **V3**. It is also not hard to see from Definition 2.4, that $\widehat{\varphi}_i(v), \widehat{\varepsilon}_i(v) \in 2\mathbb{Z}$ for $v \in \mathcal{V}$ and $1 \leqslant i < r$, proving **V2**. □

An example of the virtual crystal construction for $\mathcal{B}_{\mathsf{spin}}$ is given in Fig. 3. The virtual crystal of this section also follows from [18]. An affine version of this virtual crystal construction (which implies the one in this section) has appeared in [10, Lemma 4.2].

2.2.2. Virtual crystal $B_r \hookrightarrow C_r$ vector to vector

The crystal $\mathcal{B}_{\square}$ of Definition 2.2 can be realized as a virtual crystal inside the ambient crystal $\widehat{\mathcal{V}} = \mathcal{C}_{\square}^{\otimes 2}$.

Definition 2.10. Define $\mathcal{V} \subseteq \widehat{\mathcal{V}} = \mathcal{C}_{\square}^{\otimes 2}$ of type C_r as

$$\mathcal{V} = \{a \otimes a \mid 1 \leqslant a \leqslant r\} \cup \{\overline{a} \otimes \overline{a} \mid 1 \leqslant a \leqslant r\} \cup \{r \otimes \overline{r}\}$$

with $f_i = \widehat{f}_i^2$, $e_i = \widehat{e}_i^2$ for $1 \leqslant i < r$ and $f_r = \widehat{f}_r$, $e_r = \widehat{e}_r$.

Lemma 2.11. *$\mathcal{V} \sqcup \{\emptyset\}$ of Definition 2.10 is closed under the operators f_i and e_i for $1 \leqslant i \leqslant r$ and all elements in $\mathcal{V}$ are in the connected component of $\widehat{\mathcal{V}}$ with highest weight $1 \otimes 1$.*

Proof. We leave this to the reader to check. □

Definition 2.12. Let $\Psi \colon \mathcal{B}_{\square} \to \mathcal{V}$ be the map $\Psi(a) = a \otimes a$ and $\Psi(\overline{a}) = \overline{a} \otimes \overline{a}$ for $1 \leqslant a \leqslant r$ and $\Psi(0) = r \otimes \overline{r}$.

Lemma 2.13. *The map Ψ of Definition 2.12 is a bijective map that intertwines the crystal operators on $\mathcal{B}_{\square}$ and $\mathcal{V}$.*

Please cite this article in press as: J. Pappe et al., Promotion and growth diagrams for fans of Dyck paths and vacillating tableaux, J. Algebra (2023), https://doi.org/10.1016/j.jalgebra.2023.07.038

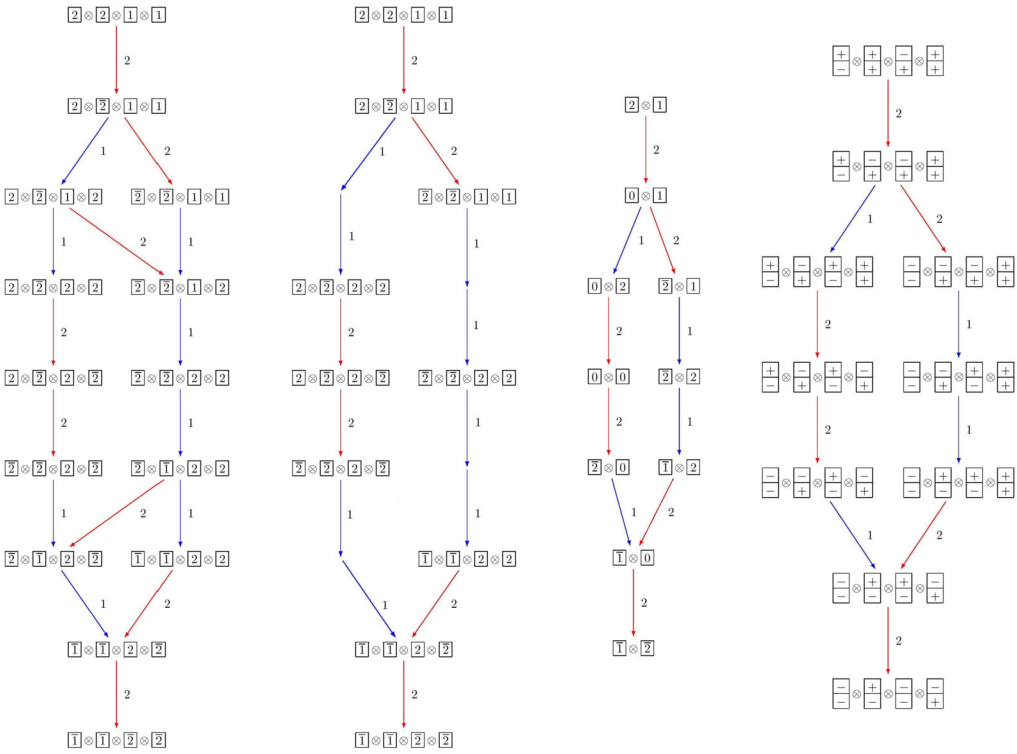

Fig. 5. Far Left: One connected component $\widehat{\mathcal{S}}$ of the crystal $\widehat{\mathcal{V}}^{\otimes 2} = (\mathcal{C}_{\square}^{\otimes 2})^{\otimes 2}$ of type C_2. Middle Left: The connected component $\mathcal{S}$ of the virtual crystal $\mathcal{V}^{\otimes 2}$ inside $\mathcal{S}$ induced by Definition 2.10. Middle Right: The corresponding connected component $\mathcal{T}$ of the crystal $\mathcal{B}_{\square}^{\otimes 2}$ of type B_2 that corresponds to $\mathcal{S}$ under the embedding given in Definition 2.12. Far Right: The connected component $\mathcal{U}$ of $(\mathcal{B}_{\mathsf{spin}} \otimes \mathcal{B}_{\mathsf{spin}})^{\otimes 2}$ of type B_2 corresponding to $\mathcal{T}$ under the isomorphism given in Fig. 6.

Proof. We leave this to the reader to check. □

Proposition 2.14. *$\mathcal{V}$ of Definition 2.10 is a virtual crystal for the embedding of Lie algebras $B_r \hookrightarrow C_r$.*

Proof. We leave this to the reader to check. □

An example of the virtual crystal construction for $\mathcal{B}_{\square}$ is given in Fig. 5. The virtual crystal of this section also follows from [18]. An affine version of this virtual crystal construction (which implies the one in this section) has appeared in [10, Theorem 4.8].

2.3. Highest weights of weight zero

A weight $\lambda \in \Lambda$ is called *minuscule* if $\langle \lambda, \alpha^{\vee} \rangle \in \{0, \pm 1\}$ for all coroots $\alpha^{\vee}$. A crystal $\mathcal{B}$ is called *minuscule* if $\mathsf{wt}(b)$ is minuscule for all $b \in \mathcal{B}$. Note that $\mathcal{B}_{\mathsf{spin}}$ is a minuscule crystal (see for example [3, Chapter 5.4]).

Please cite this article in press as: J. Pappe et al., Promotion and growth diagrams for fans of Dyck paths and vacillating tableaux, J. Algebra (2023), https://doi.org/10.1016/j.jalgebra.2023.07.038

A weight λ is called *dominant* if $\langle \lambda, \alpha_i^\vee \rangle \geqslant 0$ for all $i \in I$. Let $\Lambda^+ \subseteq \Lambda$ denote the set of all dominant weights. Except for spin weights, dominant weights can be identified with partitions, where the fundamental weight ω_h corresponds to a column of height h in the partition. A *partition* λ is a sequence $\lambda = (\lambda_1, \lambda_2, \ldots, \lambda_\ell)$ such that $\lambda_1 \geqslant \lambda_2 \geqslant \cdots \geqslant \lambda_\ell \geqslant 0$. We identify partitions that differ by trailing zeroes. That is, $(3, 2, 0, 0)$ is identified with the partition $(3, 2)$.

Let $\mathcal{B}_1, \mathcal{B}_2, \ldots, \mathcal{B}_n$ be minuscule crystals. For any highest weight element

$$u = u_n \otimes \cdots \otimes u_1 \in \mathcal{B}_n \otimes \cdots \otimes \mathcal{B}_1$$

we may bijectively associate a sequence of dominant weights $\emptyset = \mu^0, \mu^1, \ldots, \mu^n$, where $\mu^q := \sum_{i=1}^q \mathsf{wt}(u_i)$. The final weight $\mu := \mu^n$ of such a sequence is also the weight of the crystal element u. If μ is zero, u is a *highest weight element of weight zero*.

Note that the number of highest weight elements of weight zero in a tensor product of crystals is equal to the dimension of the invariant subspace, see for example [43,30].

2.3.1. Oscillating tableaux

Oscillating tableaux were introduced by Sundaram [40].

Definition 2.15 *(Sundaram [40]).* An *r-symplectic oscillating tableau* O of length n and shape μ is a sequence of partitions

$$\mathsf{O} = (\emptyset = \mu^0, \mu^1, \ldots, \mu^n = \mu)$$

such that the Ferrers diagrams of two consecutive partitions differ by exactly one cell, and each partition μ^i has at most r nonzero parts.

The r-symplectic oscillating tableaux of length n and shape μ are in bijection with highest weight elements in $\mathcal{C}_\square^{\otimes n}$ of type C_r and weight μ. This can be seen by induction on n. For $n = 1$, the only highest weight element is 1 and the only oscillating tableau is $(\emptyset, \square)$. Suppose the claim is true for $n - 1$. If $u = b \otimes u_0 \in \mathcal{C}_\square^{\otimes n}$ is highest weight, then $u_0 \in \mathcal{C}_\square^{\otimes (n-1)}$ must be highest weight and hence by induction corresponds to an oscillating tableau $(\emptyset = \mu^0, \mu^1, \ldots, \mu^{n-1})$. The element b is either an unbarred or barred letter. If b is the unbarred letter a, μ^n differs from μ^{n-1} by a box in row a. If b is the barred letter $\overline{a}$, μ^n has one less box in row a than μ^{n-1}. More precisely, for a highest weight element $b_n \otimes \cdots \otimes b_1 \in \mathcal{C}_\square^{\otimes n}$, the corresponding oscillating tableau satisfies $\mu^q = \sum_{i=1}^q \mathsf{wt}(b_i)$. This map can be reversed and it is not hard to see that the result is a highest weight element using the tensor product rule.

2.3.2. r-fans of Dyck paths

Next we relate highest weight elements of weight zero in $\mathcal{B}_{\mathsf{spin}}^{\otimes n}$ of type B_r and r-fans of Dyck paths. A *Dyck path* of length n is a path from $(0, 0)$ to $(n, 0)$ consisting of up-steps $(1, 1)$ and down-steps $(1, -1)$ which never crosses the line $y = 0$.

Please cite this article in press as: J. Pappe et al., Promotion and growth diagrams for fans of Dyck paths and vacillating tableaux, J. Algebra (2023), https://doi.org/10.1016/j.jalgebra.2023.07.038

Definition 2.16. An *r-fan of Dyck paths* F of length n is a sequence

$$\mathsf{F} = (\emptyset = \mu^0, \mu^1, \dots, \mu^n = \emptyset)$$

of partitions μ^i with at most r parts such that the Ferrers diagram of two consecutive partitions differs by exactly one cell in each part. In other words, μ^i differs from μ^{i+1} by $(\pm 1, \pm 1, \dots, \pm 1)$ for $0 \leqslant i < n$.

Example 2.17. For $r = 3$ and $n = 4$, the following is a 3-fan of Dyck paths

$$\mathsf{F} = ((000), (111), (220), (111), (000)).$$

Since $\mathcal{B}_{\mathsf{spin}}$ of type B_r is minuscule, by the above discussion $\epsilon = \epsilon_n \otimes \cdots \otimes \epsilon_1 \in \mathcal{B}_{\mathsf{spin}}^{\otimes n}$ is highest weight if and only if $\sum_{i=1}^{q} \mathsf{wt}(\epsilon_i)$ is dominant for all $1 \leqslant q \leqslant n$. Hence highest weight elements of weight zero can be identified with an r-fan of Dyck paths of length n: the j-th entry of ϵ_i is $+$ if and only if the j-th Dyck path has an up-step at position i. In particular, for a highest weight element ϵ of weight zero, the sequence of dominant weights $\mu^q := \sum_{i=1}^{q} 2\mathsf{wt}(\epsilon_i)$ for $0 \leqslant q \leqslant n$ defines an r-fan of Dyck paths consistent with Definition 2.16.

A similar bijection was given in [26].

Example 2.18. The 3-fan of Dyck paths of Example 2.17 corresponds to the element

$$\epsilon = (-,-,-) \otimes (-,-,+) \otimes (+,+,-) \otimes (+,+,+) \in \mathcal{B}_{\mathsf{spin}}^{\otimes 4}.$$

Following Definition 2.7, we obtain an embedding from the set of r-fans of Dyck paths into the set of oscillating tableaux.

Definition 2.19. For an r-fan of Dyck paths $\mathsf{F} = (\emptyset = \lambda^0, \lambda^1, \dots, \lambda^n = \emptyset)$ we define the oscillating tableau $\iota_{F \to O}(\mathsf{F}) = (\emptyset = \mu^0, \dots, \mu^{rn} = \emptyset)$ as follows. Let $v^t = \Psi(\lambda^t - \lambda^{t-1})$ for $1 \leqslant t \leqslant n$ with Ψ as in Definition 2.7. Then

$$\mu^{tr+s} = \lambda^t + \sum_{i=1}^{s} \mathsf{wt}(v_i^{t+1}) \qquad \text{for } 0 \leqslant t < n,\ 0 \leqslant s < r.$$

2.3.3. Vacillating tableaux

Next we define *vacillating tableaux* which correspond to highest weight elements in $\mathcal{B}_{\square}^{\otimes n}$ of type B_r.

Definition 2.20. A *$(2r+1)$-orthogonal vacillating tableau* of length n is a sequence of partitions $\mathsf{V} = (\emptyset = \lambda^0, \dots, \lambda^n)$ such that:

(i) λ^i has at most r parts.

Please cite this article in press as: J. Pappe et al., Promotion and growth diagrams for fans of Dyck paths and vacillating tableaux, J. Algebra (2023), https://doi.org/10.1016/j.jalgebra.2023.07.038

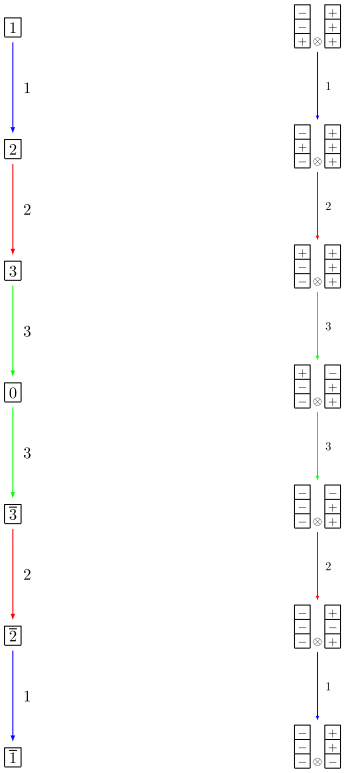

Fig. 6. Left: $\mathcal{B}_{\square}$ of type B_3, Right: The component in $\mathcal{B}_{\mathsf{spin}} \otimes \mathcal{B}_{\mathsf{spin}}$ of type B_3 isomorphic to $\mathcal{B}_{\square}$.

(ii) Two consecutive partitions either differ by a box or are equal.
(iii) If two consecutive partitions are equal, then all their r parts are greater than 0.

We call λ^n the *weight* of V.

A highest weight element $u = u_n \otimes \cdots \otimes u_1 \in \mathcal{B}_{\square}^{\otimes n}$ of type B_r corresponds to the $(2r+1)$-vacillating tableau $(\emptyset = \lambda^0, \lambda^1, \ldots, \lambda^n)$, where $\lambda^q = \sum_{i=1}^{q} \mathsf{wt}(u_i)$.

Note that $\mathcal{B}_{\square}$ is not minuscule. The crystal $\mathcal{B}_{\square}$ is isomorphic to the component with highest weight element $(+,-,\ldots,-) \otimes (+,\ldots,+)$ in $\mathcal{B}_{\mathsf{spin}} \otimes \mathcal{B}_{\mathsf{spin}}$, see Fig. 6. From this we obtain a map from the set of vacillating tableaux of weight zero and length n into the set of fans of Dyck paths of length $2n$ that we now explain. Denote by $\mathbf{1}$ the vector $\mathbf{e}_1 + \mathbf{e}_2 + \cdots + \mathbf{e}_r$ and write $\rho < \nu$ if $\nu = \rho + \mathbf{e}_i$ for some i.

Definition 2.21. For a vacillating tableau of weight zero $\mathsf{V} = (\emptyset = \lambda^0, \ldots, \lambda^n = \emptyset)$ we define the fan of Dyck paths $\iota_{V \to F}(\mathsf{V}) = (\emptyset = \mu^0, \ldots, \mu^{2n} = \emptyset)$ as follows:

$$\mu^{2i} = 2 \cdot \lambda^i$$

Please cite this article in press as: J. Pappe et al., Promotion and growth diagrams for fans of Dyck paths and vacillating tableaux, J. Algebra (2023), https://doi.org/10.1016/j.jalgebra.2023.07.038

$$\mu^{2i-1} = \begin{cases} 2 \cdot \lambda^{i-1} + \mathbf{1} & \text{if } \lambda^{i-1} < \lambda^i, \\ 2 \cdot \lambda^i + \mathbf{1} & \text{if } \lambda^{i-1} > \lambda^i, \\ 2 \cdot \lambda^{i-1} + \mathbf{1} - 2\mathbf{e}_r & \text{if } \lambda^{i-1} = \lambda^i. \end{cases}$$

Similarly, following Definition 2.12, we obtain an embedding from the set of vacillating tableaux of weight zero into the set of oscillating tableaux.

Definition 2.22. For a vacillating tableau of weight zero $\mathsf{V} = (\emptyset = \lambda^0, \dots, \lambda^n = \emptyset)$ we define the oscillating tableau $\iota_{V \to O}(\mathsf{V}) = (\emptyset = \mu^0, \dots, \mu^{2n} = \emptyset)$ as follows:

$$\mu^{2i} = 2 \cdot \lambda^i$$
$$\mu^{2i-1} = \lambda^{i-1} + \lambda^i + \begin{cases} 0 & \text{if } \lambda^{i-1} \neq \lambda^i, \\ -\mathbf{e}_r & \text{if } \lambda^{i-1} = \lambda^i. \end{cases}$$

2.4. Promotion via crystal commutor

For finite crystals B_λ of classical type of highest weight λ, Henriques and Kamnitzer [12] introduced the crystal commutor as follows. Let $\eta_{B_\lambda} \colon B_\lambda \to B_\lambda$ be the Lusztig involution, which maps the highest weight vector to the lowest weight vector and interchanges the crystal operators f_i with $e_{i'}$, where $w_0(\alpha_i) = -\alpha_{i'}$ under the longest element w_0. This can be extended to tensor products of such crystals by mapping each connected component to itself using the above. Then the *crystal commutor* is defined as

$$\begin{aligned} \sigma \colon B_\lambda \otimes B_\mu &\to B_\mu \otimes B_\lambda \\ b \otimes c &\mapsto \eta_{B_\mu \otimes B_\lambda}(\eta_{B_\mu}(c) \otimes \eta_{B_\lambda}(b)). \end{aligned}$$

If we want to emphasize the crystals involved, we write $\sigma_{A,B} \colon A \otimes B \to B \otimes A$.

Following [7,43,44], we define the promotion operator using the crystal commutor.

Definition 2.23. Let C be a crystal and $u \in C^{\otimes n}$ a highest weight element. Then *promotion* pr on u is defined as $\sigma_{C^{\otimes n-1},C}(u)$.

Remark 2.24. Note that inverse promotion is given by $\sigma_{C,C^{\otimes n-1}}(u)$. The conventions in the literature about what is called promotion and what is called inverse promotion are not always consistent. Our convention here agrees with the definition of promotion on posets that removes the letters 1 and slides letters (see for example [38,2]). The convention here is the opposite of the convention on tableaux which removes the largest letter and uses jeu de taquin slides (see for example [31,4]).

Example 2.25. Consider the crystal $C = B_{\square}$ of type A_2 (see [3]). Then

$$u = 1 \otimes 3 \otimes 2 \otimes 2 \otimes 1 \otimes 1 \in C^{\otimes 6}$$

Please cite this article in press as: J. Pappe et al., Promotion and growth diagrams for fans of Dyck paths and vacillating tableaux, J. Algebra (2023), https://doi.org/10.1016/j.jalgebra.2023.07.038

is highest weight and

$$\sigma_{C^{\otimes 5},C}(u) = 2 \otimes 1 \otimes 3 \otimes 1 \otimes 2 \otimes 1.$$

The recording tableaux for the RSK insertion of the words 132211 and 213121 (from right to left) are

1	2	6
3	4	
5		

and

1	3	5
2	6	
4		

which are related by the usual (inverse) promotion operator (removing the letter 1, doing jeu-de-taquin slides, filling the empty cell with the largest letter plus one and subtracting 1 from all entries) on standard tableaux.

Example 2.26. Promotion on the element ϵ in Example 2.18 is

$$\sigma_{\mathcal{B}_{\text{spin}}^{\otimes 3},\mathcal{B}_{\text{spin}}}(\epsilon) = (-,-,-) \otimes (-,+,+) \otimes (+,-,-) \otimes (+,+,+).$$

Note that if $\Psi\colon C \to \mathcal{V} \subseteq \widehat{\mathcal{V}}$ is a virtual embedding, then virtualization intertwines with promotion

$$\Psi \circ \sigma_{C^{\otimes n-1},C} = \sigma_{\widehat{\mathcal{V}}^{\otimes n-1},\widehat{\mathcal{V}}} \circ \Psi \tag{2.3}$$

by Axioms V2 and V3 in Definition 2.3 as long as the folding σ and the multiplication factors γ_i respect the map $w_0(\alpha_i) = -\alpha_{i'}$. This is the case for the virtualizations in this paper.

2.5. Promotion via local rules

Adapting local rules of van Leeuwen [41], Lenart [23] gave a combinatorial realization of the crystal commutor $\sigma_{A,B}$ by constructing an equivalent bijection between the highest weight elements of $A \otimes B$ and $B \otimes A$ respectively. The *local rules* of Lenart [23] can be stated as follows: four weight vectors $\lambda, \mu, \kappa, \nu \in \Lambda$ depicted in a square diagram

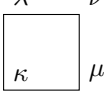

satisfy the local rule, if $\mu = \mathrm{dom}_W(\kappa + \nu - \lambda)$, where W is the Weyl group of the root system Φ underlying A and B. Furthermore, $\mathrm{dom}_W(\rho)$ is the dominant weight in the Weyl orbit of ρ.

Theorem 2.27 *([23, Theorem 4.4]). Let A and B be crystals embedded into tensor products $A_\ell \otimes \cdots \otimes A_1$ and $B_k \otimes \cdots \otimes B_1$ of crystals of minuscule representations, respectively.*

Please cite this article in press as: J. Pappe et al., Promotion and growth diagrams for fans of Dyck paths and vacillating tableaux, J. Algebra (2023), https://doi.org/10.1016/j.jalgebra.2023.07.038

Let $w = w_{k+\ell} \otimes \cdots \otimes w_1$ be a highest weight element in $A \otimes B$ with corresponding tableau $(\emptyset = \mu^0, \mu^1, \ldots, \mu^{k+\ell} = \mu)$ Then $\sigma_{A,B}(w)$ can be computed as follows. Create a $k \times \ell$ grid of squares as in (2.4), labeling the edges along the left border with $w_1, \ldots, w_k$ and the edges along the top border with $w_{k+1}, \ldots, w_{k+\ell}$:

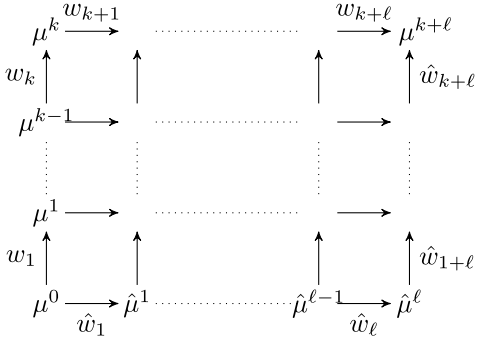

(2.4)

For each square use the local rule to compute the weight vectors on the square's corners. Given a horizontal edge from κ to μ in the jth column, label the edge by the element in A_j with weight $\mu - \kappa$. Similarly, given a vertical edge from μ to ν in the ith row, label the edge by the element in B_i with weight $\nu - \mu$. The labels $\hat{w}_{k+\ell} \ldots \hat{w}_1$ of the edges along the right and the bottom border of the grid then form $\sigma_{A,B}(w)$ with corresponding tableau $(\emptyset = \mu^0, \hat{\mu}^1, \ldots, \hat{\mu}^{k+\ell-1}, \mu^{k+\ell} = \mu)$.

Example 2.28. Performing Lenart's local rules on the elements in Example 2.25 gives

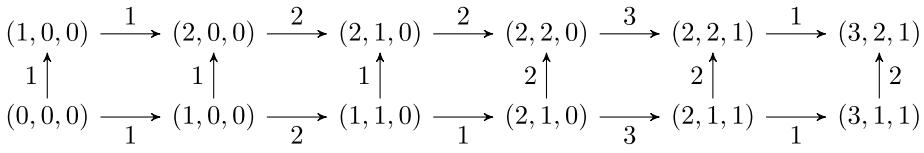

which recovers $\sigma_{C^{\otimes 5},C}(1 \otimes 3 \otimes 2 \otimes 2 \otimes 1 \otimes 1) = 2 \otimes 1 \otimes 3 \otimes 1 \otimes 2 \otimes 1$.

3. Chord diagrams

3.1. Promotion matrices

In this section we describe a map from highest weight words of weight zero to chord diagrams that intertwines promotion and rotation.

We start with the definition of chord diagrams and their rotation.

Definition 3.1. A *chord diagram* of size n is a graph with n vertices depicted on a circle which are labeled $1, \ldots, n$ in counter-clockwise orientation.

Please cite this article in press as: J. Pappe et al., Promotion and growth diagrams for fans of Dyck paths and vacillating tableaux, J. Algebra (2023), https://doi.org/10.1016/j.jalgebra.2023.07.038

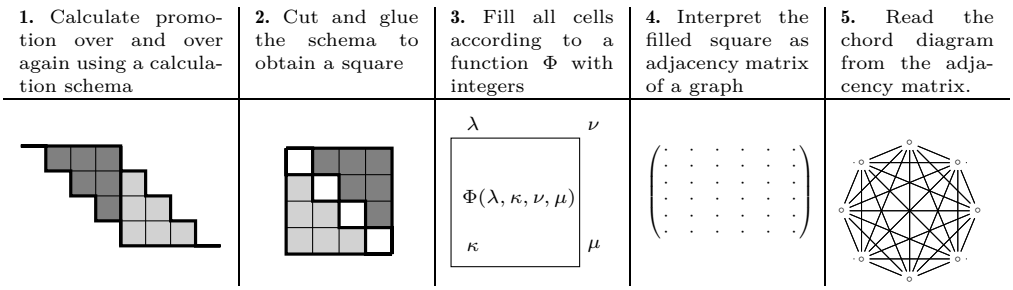

Fig. 7. Overview of the steps in our map.

The *rotation* of a chord diagram is obtained by rotating all edges clockwise by $\frac{2\pi}{n}$ around the center of the diagram.

In our setting all chord diagrams are undirected graphs with possibly multiple edges between the same two vertices. We can therefore identify chord diagrams with their *adjacency matrix*. The adjacency matrix is a symmetric $n \times n$ matrix $M = (m_{ij})_{1 \leqslant i,j \leqslant n}$ with non-negative integer entries and m_{ij} denotes the number of edges between vertex i and vertex j.

Proposition 3.2. *Let M be the adjacency matrix of a chord diagram G. Denote by* $\operatorname{rot} M$ *the toroidal shift of M, that is, the matrix obtained from M by first cutting the top row and pasting it to the bottom and then cutting the leftmost column and pasting it to the right.*

Then $\operatorname{rot} M$ *is the adjacency matrix corresponding to the rotation of G.*

The proof of this proposition is easy and left to the reader as an exercise.

Let us now outline the idea to construct such a rotation and promotion intertwining map and then provide the details on the individual steps on the examples of oscillating tableaux, r-fans of Dyck paths and vacillating tableaux. A visual guideline can be seen in Fig. 7.

Construction 3.3. The construction is given as follows:

Step 1: Iteratively calculate promotion of a highest weight word of weight zero and length n using Lenart's schema (2.4) a total of n times.
Step 2: Group the results into a square grid, called the *promotion matrix*.
Step 3: Fill the cells of the square grid with certain non-negative integers according to a filling rule Φ that only depends on the four corners of the cells in the schema (2.4).
Step 4: Regard the filling as the adjacency matrix of a graph, which is the chord diagram.

We now discuss the filling rules in the various cases. Note that the filling rules are new even in the case of oscillating tableaux as the proofs in [30] did not follow this construction.

Please cite this article in press as: J. Pappe et al., Promotion and growth diagrams for fans of Dyck paths and vacillating tableaux, J. Algebra (2023), https://doi.org/10.1016/j.jalgebra.2023.07.038

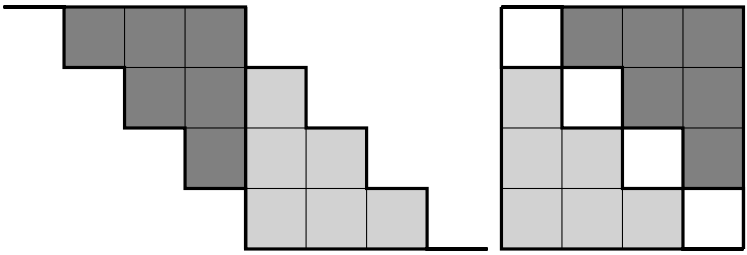

Fig. 8. The transformation into a promotion matrix. The highlighted part is cut away and glued on the left.

3.1.1. Chord diagrams for oscillating tableaux

Recall that the Weyl group of type C_r is the hyperoctahedral group $\mathfrak{H}_r$ of signed permutations of $\{\pm 1, \pm 2, \ldots, \pm r\}$. Weights are elements in $\mathbb{Z}^r$ and dominant weights are weakly decreasing integer vectors with non-negative entries (or equivalently partitions). Thus, the dominant representative $\mathrm{dom}_{\mathfrak{H}_r}(\lambda)$ of a weight λ is obtained by sorting the absolute values of its entries into weakly decreasing order.

We slightly modify Lenart's schema for the crystal commutor (2.4) by omitting edge labels as only the weights on the corners are needed. Additionally, given an oscillating tableau $\mathsf{O} = (\emptyset = \mu^0, \mu^1, \ldots, \mu^n = \mu)$, we start each row with the zero weight $\emptyset$ and end each row with the weight μ, which makes it easier to iteratively use this schema to calculate promotion. This way the promotion of the oscillating tableau $\mathsf{O} = (\emptyset = \mu^0, \mu^1, \ldots, \mu^n = \mu)$ is the unique sequence $(\emptyset = \hat{\mu}^0, \hat{\mu}^1, \ldots, \hat{\mu}^n = \mu)$, such that all squares in the diagram

satisfy the local rule of Section 2.5.

Using this schema we iteratively calculate promotion a total of n times and depict the results in a diagram as seen in Fig. 8 on the left. This diagram consists of n promotion schemas glued together. As $\mathsf{pr}^n = \mathsf{id}$, the labels on the top and the bottom row must be equal to $\mu^0, \ldots, \mu^n$.

We now transform this diagram by copying everything to the right of the n-th column into the triangular empty space on the left, see Fig. 8. In this way the labels on the right corners of the n-th column are duplicated. We obtain an $n \times n$ grid, where each corner of a cell is labeled with a dominant weight and the labels on the top and bottom border are equal and the labels on the left and right border are equal. This grid is called the *promotion matrix* of O.

Please cite this article in press as: J. Pappe et al., Promotion and growth diagrams for fans of Dyck paths and vacillating tableaux, J. Algebra (2023), https://doi.org/10.1016/j.jalgebra.2023.07.038

To obtain an adjacency matrix, we fill the cells of this diagram with non-negative integers according to the following rule.

Definition 3.4. The *filling rule* for oscillating tableaux is

$$\Phi(\lambda, \kappa, \nu, \mu) = \begin{cases} 1 & \text{if } \kappa + \nu - \lambda \text{ contains a negative entry,} \\ 0 & \text{else,} \end{cases} \tag{3.1}$$

where the cells are labeled as depicted below:

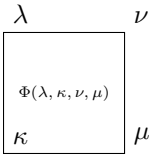

(3.2)

Definition 3.5. Denote by M_O the function that maps an r-symplectic oscillating tableau of length n to an $n \times n$ adjacency matrix using Construction 3.3 and the filling rule (3.1).

Next, we generalize the above construction for r-fans of Dyck paths and vacillating tableaux.

3.1.2. Chord diagrams for r-fans of Dyck paths

Given an r-fan of Dyck paths $\mathsf{F} = (\emptyset = \mu^0, \mu^1, \ldots, \mu^n = \emptyset)$, we construct an adjacency matrix via Construction 3.3 using the following filling rule:

Definition 3.6. The *filling rule* for fans of Dyck paths is

$$\Phi(\lambda, \kappa, \nu, \mu) = \text{number of negative entries in } \kappa + \nu - \lambda, \tag{3.3}$$

where the cells are labeled as in (3.2).

Remark 3.7. Note that for oscillating tableaux at most one negative entry can occur. Thus the filling rule (3.3) for fans of Dyck paths is a natural generalization of the rule (3.1).

Definition 3.8. Denote by M_F the function that maps an r-fan of Dyck paths of length n to an $n \times n$ adjacency matrix using Construction 3.3 and the filling rule (3.3).

Example 3.9. Consider the following fan corresponding to the sequence of vectors $\mathsf{F} = (000, 111, 222, 311, 422, 331, 222, 111, 000)$.

Please cite this article in press as: J. Pappe et al., Promotion and growth diagrams for fans of Dyck paths and vacillating tableaux, J. Algebra (2023), https://doi.org/10.1016/j.jalgebra.2023.07.038

(1) We apply promotion a total of $n = 8$ times, to obtain the full orbit.

```
000 111 222 311 422 331 222 111 000
    000 111 200 311 220 111 000 111 000
        000 111 222 311 220 111 222 111 000
            000 111 200 111 200 311 200 111 000
                000 111 220 311 422 311 222 111 000
                    000 111 220 331 220 311 200 111 000
                        000 111 222 111 220 111 220 111 000
                            000 111 000 111 200 311 220 111 000
                                000 111 222 311 422 331 222 111 000.
```

(2) We group the results into the promotion matrix and fill the cells of the square grid according to Φ. For better readability we omitted zeros.

000	111	222	311	422	331	222	111	000
								3
111	000	111	200	311	220	111	000	111
		2				**1**		
222	111	000	111	222	311	220	111	222
	2				**1**			
311	200	111	000	111	200	111	200	311
			2		**1**			
422	311	222	111	000	111	220	311	422
			2		**1**			
331	220	311	200	111	000	111	220	331
		1		**1**		**1**		
222	111	220	111	220	111	000	111	222
	1		**1**		**1**			
111	000	111	200	311	220	111	000	111
3								
000	111	222	311	422	331	222	111	000

(3) Regard the filling as the adjacency matrix of a graph, the chord diagram.

$$\mathsf{M}_F(\mathsf{F}) = \begin{pmatrix} 0&0&0&0&0&0&0&3 \\ 0&0&2&0&0&0&1&0 \\ 0&2&0&0&0&1&0&0 \\ 0&0&0&0&2&0&1&0 \\ 0&0&0&2&0&1&0&0 \\ 0&0&1&0&1&0&1&0 \\ 0&1&0&1&0&1&0&0 \\ 3&0&0&0&0&0&0&0 \end{pmatrix}$$

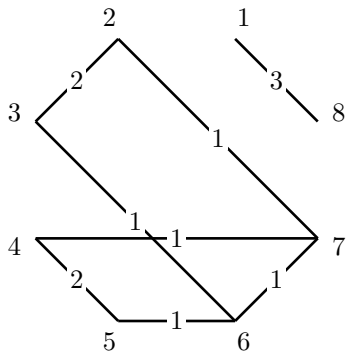

3.1.3. Chord diagrams for vacillating tableaux

Note that $\mathcal{B}_\square$ is not minuscule and thus Theorem 2.27 is not directly applicable. Using Definition 2.12 we can embed $\mathcal{B}_\square$ in $\mathcal{C}_\square^{\otimes 2}$ which gives a map $\iota_{V\to O}$ from vacillating tableaux to oscillating tableaux of twice the length which commutes with the crystal commutor. That is

Please cite this article in press as: J. Pappe et al., Promotion and growth diagrams for fans of Dyck paths and vacillating tableaux, J. Algebra (2023), https://doi.org/10.1016/j.jalgebra.2023.07.038

$$\iota_{V\to O}\circ \mathsf{pr}_{\mathcal{B}_\square} = \iota_{V\to O}\circ \sigma_{\mathcal{B}_\square^{\otimes n-1},\mathcal{B}_\square} = \sigma_{(\mathcal{C}_\square^{\otimes 2})^{\otimes n-1},\mathcal{C}_\square^{\otimes 2}}\circ \iota_{V\to O}. \tag{3.4}$$

This follows directly from the properties of virtualization.

Let V be a vacillating tableau of length n and weight zero. Let $\mathsf{O} = (\emptyset = \mu^0, \mu^1, \ldots, \mu^{2n} = \emptyset)$ be the corresponding oscillating tableau using $\iota_{V\to O}$. Then we obtain the promotion of V using the following schema

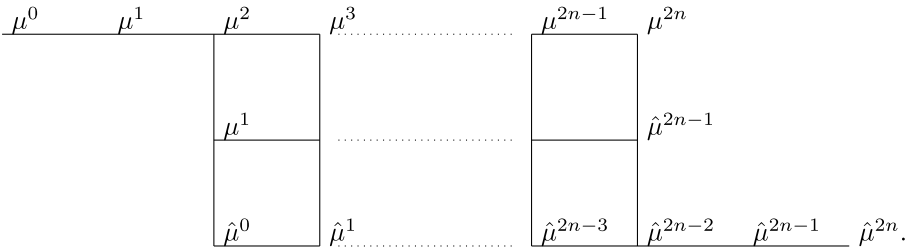

(3.5)

Following Construction 3.3, we apply promotion a total of n times and use the cut-and-glue procedure to obtain a $2n \times 2n$ square. We fill the squares using the filling rule for oscillating tableaux as given by (3.1).

To obtain an $n \times n$ adjacency matrix, we subdivide the $2n \times 2n$ matrix into 2×2 blocks and take the sum of each block.

Definition 3.10. Denote by $\mathsf{M}_{V\to O}$ the function that maps a vacillating tableau V of weight zero of length n to an $n \times n$ adjacency matrix using $\iota_{V\to O}$, Schema (3.5), Construction 3.3, filling rule (3.1), and block sums.

Example 3.11. Consider the vacillating tableau of length 9

$$\mathsf{V} = (000, 100, 200, 210, 211, 111, 111, 110, 100, 000).$$

We first embed V into an oscillating tableau using the bijection Ψ from $\mathcal{B}_\square$ to $\mathcal{V}$ given in Definition 2.12. Specifically, we use Ψ to establish a correspondence between the highest weight element in $\mathcal{B}_\square^{\otimes 9}$ associated to V and a highest weight element in $(\mathcal{C}_\square^{\otimes 2})^{\otimes 9}$, from which we obtain $\iota_{V\to O}(\mathsf{V})$ as

$$\iota_{V\to O}(\mathsf{V}) = (000, 100, 200, 300, 400, 410, 420, 421, 422, 322, 222, 221,$$
$$222, 221, 220, 210, 200, 100, 000).$$

(1) We apply promotion a total of $n = 9$ times on the above schema ($2n = 18$ times on the oscillating tableau $\iota_{V\to O}(\mathsf{V})$), to obtain the full orbit. Below the first iteration of promotion, we show all 9 applications of promotion.

000	100	200	300	400	410	420	421	422	322	222	221	222	221	220	210	200	100	000
		100	200	300	310	320	321	322	222	221	220	221	220	221	211	210	110	100
		000	100	200	210	220	221	222	221	220	221	222	221	222	221	220	210	200	100	000

Please cite this article in press as: J. Pappe et al., Promotion and growth diagrams for fans of Dyck paths and vacillating tableaux, J. Algebra (2023), https://doi.org/10.1016/j.jalgebra.2023.07.038

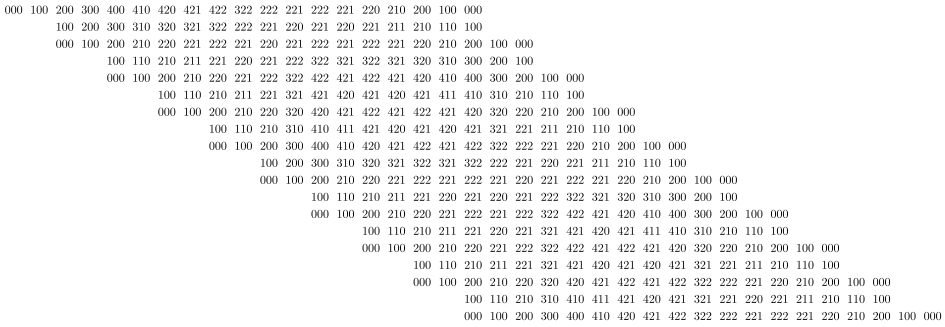

(2) We group the results into the promotion matrix and fill the cells of the square grid according to Φ in (3.1). For better readability, we subdivided the diagram into 2×2 blocks and took the sum of the entries in each block, as well as omitted the zeros.

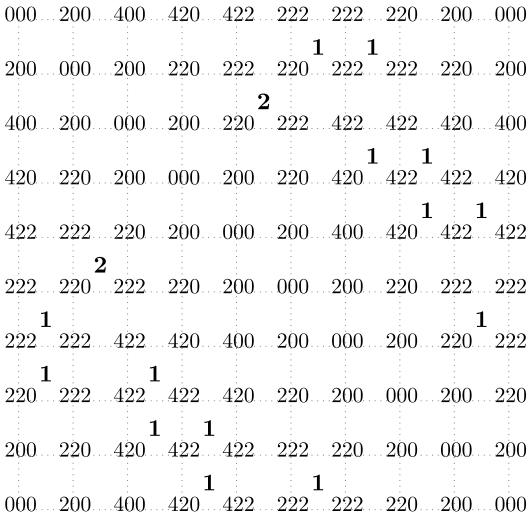

(2) Regard the filling as the adjacency matrix of a graph, the chord diagram.

$$\mathsf{M}_{V\to O}(\mathsf{V}) = \begin{pmatrix} 0&0&0&0&0&1&1&0&0\\ 0&0&0&0&2&0&0&0&0\\ 0&0&0&0&0&0&1&1&0\\ 0&0&0&0&0&0&0&1&1\\ 0&2&0&0&0&0&0&0&0\\ 1&0&0&0&0&0&0&0&1\\ 1&0&1&0&0&0&0&0&0\\ 0&0&1&1&0&0&0&0&0\\ 0&0&0&1&0&1&0&0&0 \end{pmatrix}$$

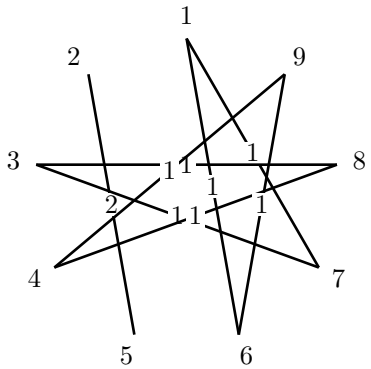

Please cite this article in press as: J. Pappe et al., Promotion and growth diagrams for fans of Dyck paths and vacillating tableaux, J. Algebra (2023), https://doi.org/10.1016/j.jalgebra.2023.07.038

Alternatively, we may obtain an adjacency matrix by embedding $\mathcal{B}_\square$ as a connected component of $\mathcal{B}_{\mathsf{spin}}^{\otimes 2}$ (see Section 2.3.3). As discussed in Definition 2.21, this embedding gives rise to the map $\iota_{V\to F}$ from vacillating tableaux to r-fans of Dyck paths of twice the length. From the r-fans of Dyck paths, we apply M_F to obtain a $2n \times 2n$ matrix. Subdividing this matrix into 2×2 blocks and taking block sums produces an $n \times n$ adjacency matrix for vacillating tableaux.

Definition 3.12. Denote by $\mathsf{M}_{V\to F}$ the function that maps a vacillating tableau V of weight zero and length n to an $n \times n$ adjacency matrix using $\iota_{V\to F}$, Construction 3.3, filling rule (3.3), and block sums.

3.1.4. Promotion and rotation

For the various maps M_X with $X \in \{O, F, V \to O, V \to F\}$ constructed in this section, we obtain the following main result.

Proposition 3.13. *The map* M_X *for* $X \in \{O, F, V \to O, V \to F\}$ *intertwines promotion and rotation, that is*

$$\mathsf{M}_X \circ \mathsf{pr} = \mathrm{rot} \circ \mathsf{M}_X.$$

Proof. Let T be either a fan of Dyck paths, an oscillating tableau of weight zero or a vacillating tableau of weight zero of length n and denote by $\widehat{\mathsf{T}}$ its promotion.

For $0 \leqslant i, j < n$ let $\mu^{i,j}$ be the $(j-i)$-th entry of $\mathsf{pr}^i(\mathsf{T})$, where indexing starts with zero and is understood modulo n. For $1 \leqslant i, j \leqslant n$ denote by $m_{i,j}$ the entry in the i-th row and j-th column of $\mathsf{M}_X(\mathsf{T})$. Similarly, denote by $\widehat{\mu}^{i,j}$ the $(j-i)$-th entry of $\mathsf{pr}^i(\widehat{\mathsf{T}})$ and by $\widehat{m}_{i,j}$ the i-th row and j-th column of $\mathsf{M}_X(\widehat{\mathsf{T}})$.

In all of our constructions $m_{i,j}$ depends on the four partitions $\mu^{i-1,j-1}$, $\mu^{i,j-1}$, $\mu^{i-1,j}$ and $\mu^{i,j}$ via some function $m_{i,j} = \widetilde{\Phi}(\mu^{i-1,j-1}, \mu^{i,j-1}, \mu^{i-1,j}, \mu^{i,j})$. Analogously we have $\widehat{m}_{i,j} = \widetilde{\Phi}(\widehat{\mu}^{i-1,j-1}, \widehat{\mu}^{i,j-1}, \widehat{\mu}^{i-1,j}, \widehat{\mu}^{i,j})$.

A simple calculation gives

$$\begin{aligned}\widehat{m}_{i,j} &= \widetilde{\Phi}(\widehat{\mu}^{i-1,j-1}, \widehat{\mu}^{i,j-1}, \widehat{\mu}^{i-1,j}, \widehat{\mu}^{i,j}) \\ &= \widetilde{\Phi}(\mu^{i,j}, \mu^{i+1,j}, \mu^{i,j+1}, \mu^{i+1,j+1}) = m_{i+1,j+1},\end{aligned}$$

where indices are understood modulo n. Thus, $\mathsf{M}_X(\widehat{\mathsf{T}}) = \mathrm{rot}(\mathsf{M}_X(\mathsf{T}))$. □

Note that the promotion matrix $\mathsf{M}_X(\mathsf{T})$ is sometimes referred to as the *promotion-evacuation diagram* of T as it also encodes information about the evacuation of T. Following [30], a generalization of Schützenberger's evacuation operator can be defined on crystals as follows.

Definition 3.14. Let C be a crystal and $u \in C^{\otimes n}$ a highest weight element. Then *evacuation* evac on u is defined as

$$(1_{C^{\otimes n-2}} \otimes \mathsf{pr}) \circ \cdots \circ (1_C \otimes \mathsf{pr}) \circ \mathsf{pr}(u),$$

where $(1_{C^{\otimes n-m}} \otimes \mathsf{pr})(w_n \otimes \cdots \otimes w_2 \otimes w_1) = w_n \otimes \cdots \otimes w_{m+1} \otimes \mathsf{pr}(w_m \otimes \cdots \otimes w_1)$.

Given a tableau T corresponding to a highest weight element u, we denote by $\mathsf{evac}(\mathsf{T})$ the tableau associated to the highest weight element $\mathsf{evac}(u)$.

Proposition 3.15. *The map* M_X *for* $X \in \{O, F, V \to O, V \to F\}$ *intertwines evacuation and the anti-transpose, that is*

$$\mathsf{M}_X \circ \mathsf{evac} = \mathrm{antr} \circ \mathsf{M}_X,$$

where the anti-transpose antr *of a matrix is its transpose over its anti-diagonal.*

Proof. Let T be either a fan of Dyck paths, an oscillating tableau of weight zero, or a vacillating tableau of weight zero of length n. From the definition of evac and the construction of M_X, we have that $\mathsf{evac}(\mathsf{T})$ is precisely the tableau obtained by reading the right border of M_X from bottom to top. Note that in order to prove the statement for $\mathsf{M}_{V\to O}$ it suffices to show it for M_O as Ψ intertwines $\sigma_{\mathcal{B}_\square^{\otimes m}, \mathcal{B}_\square}$ and $\sigma_{(\mathcal{C}_\square^{\otimes 2})^{\otimes m}, \mathcal{C}_\square^{\otimes 2}}$ for all $m \geqslant 1$ by Equation (2.3), where Ψ is the virtualization map given in Definition 2.12. Similarly, in order to prove the statement for $\mathsf{M}_{V\to F}$ it suffices to prove it for M_F.

Consider partitions $\lambda, \kappa, \nu, \mu$ labeling the corner of a cell in M_X as in (3.2), where $X \in \{O, F\}$. By [41, Lemma 4.1.2], we have $\mu = \mathrm{dom}_W(\kappa + \nu - \lambda)$ if and only if $\lambda = \mathrm{dom}_W(\kappa + \nu - \mu)$ as $\mathcal{B}_{\mathsf{spin}}$ and $\mathcal{C}_\square$ are minuscule. This implies that partitions labeling the corners of every cell in $\mathsf{M}_X \circ \mathsf{evac}$ and $\mathrm{antr} \circ \mathsf{M}_X$ are equal.

To complete the proof we show that filling rules $\Phi(\lambda, \kappa, \nu, \mu)$ given in (3.1) and (3.3) satisfy $\Phi(\lambda, \kappa, \nu, \mu) = \Phi(\mu, \kappa, \nu, \lambda)$. As partitions connected by a vertical or horizontal edge in M_O differ by exactly one box, we have that $\Phi(\lambda, \kappa, \nu, \mu) = 1$ if and only if $\lambda = \mu = (\lambda_1, \ldots, \lambda_i, 0, \ldots, 0)$, $\lambda_i = 1$ for some i, and $\kappa = \nu = (\lambda_1, \ldots, \lambda_{i-1}, 0, 0, \ldots, 0)$. Thus, the filling rule for oscillating tableaux satisfies $\Phi(\lambda, \kappa, \nu, \mu) = \Phi(\mu, \kappa, \nu, \lambda)$. By a similar argument the filling rule for fans of Dyck paths also satisfies the desired symmetry. □

3.2. Fomin growth diagrams

Generally speaking, a *Fomin growth diagram* is a means to bijectively map sequences of partitions satisfying certain constraints to fillings of a Ferrers shape with non-negative integers [9,32,42,21]. In this setting, we draw the Ferrers shape in French notation (to fix how the growth diagrams are arranged).

To map a filling of a Ferrers shape to a sequence of partitions we iteratively label all corners of cells of the shape with partitions by certain local rules. Given a cell, where already all three partitions on the left and bottom corners are known, the forward rules determine the fourth partition on the top right corner based on the filling of the cell. Conversely, given the three partitions on the top and right corners of a cell, the backwards

Please cite this article in press as: J. Pappe et al., Promotion and growth diagrams for fans of Dyck paths and vacillating tableaux, J. Algebra (2023), https://doi.org/10.1016/j.jalgebra.2023.07.038

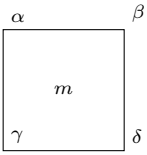

Fig. 9. A cell of a growth diagram filled with a non-negative integer m.

rules determine the last partition and the filling of the cell. When defining the local rules we label the cells as seen in Fig. 9.

For partitions δ and α, we define their union $\delta \cup \alpha$ to be the partition containing $\delta_i + \alpha_i$ cells in row i, where δ_i and α_i denote the number of cells in row i of δ and α respectively. Recall that we pad partitions with 0's if necessary. We denote $\delta \cup \delta$ by 2δ. We define the intersection of two partitions $\delta \cap \alpha$ to be the partition containing $\min\{\delta_i, \alpha_i\}$ cells in row i.

We begin by describing the local rules for a filling of a Ferrers shape with at most one 1 in each row and in each column and 0's everywhere else (omitted for readability). Moreover, we require that any two adjacent partitions in the labeling of our growth diagram (for example, $\gamma \to \alpha$ and $\gamma \to \delta$ in Fig. 9) must either coincide or the one at the head of the arrow is obtained from the other by adding a unit vector. We record the local forward rules and local backward rules for this case of 0/1 filling, which are stated explicitly in [21, p. 4-5].

Given a 0/1 filling of a Ferrers shape and partitions labeling the bottom and left side of the Ferrers shape, we apply the following *local forward rules* to complete the labeling.

(F1) If $\gamma = \delta = \alpha$, and there is no 1 in the cell, then $\beta = \gamma$.
(F2) If $\gamma = \delta \neq \alpha$, then $\beta = \alpha$.
(F3) If $\gamma = \alpha \neq \delta$, then $\beta = \delta$.
(F4) If γ, δ, α are pairwise different, then $\beta = \delta \cup \alpha$.
(F5) If $\gamma \neq \delta = \alpha$, then β is formed by adding a square to the $(k+1)$-st row of $\delta = \alpha$, given that $\delta = \alpha$ and γ differ in the k-th row.
(F6) If $\gamma = \delta = \alpha$, and if there is a 1 in the cell, then β is formed by adding a square to the first row of $\gamma = \delta = \alpha$.

Given a Ferrers shape and partitions labeling the top and right side, we apply the following *local backward rules* to complete the labeling and recover the filling.

(B1) If $\beta = \delta = \alpha$, then $\gamma = \beta$.
(B2) If $\beta = \delta \neq \alpha$, then $\gamma = \alpha$.
(B3) If $\beta = \alpha \neq \delta$, then $\gamma = \delta$.
(B4) If β, δ, α are pairwise different, then $\gamma = \delta \cap \alpha$.
(B5) If $\beta \neq \delta = \alpha$, then γ is formed by deleting a square from the $(k-1)$-st row of $\delta = \alpha$, given that $\delta = \alpha$ and β differ in the k-th row with $k \geqslant 2$.

Please cite this article in press as: J. Pappe et al., Promotion and growth diagrams for fans of Dyck paths and vacillating tableaux, J. Algebra (2023), https://doi.org/10.1016/j.jalgebra.2023.07.038

(B6) If $\beta \neq \delta = \alpha$, and if β and $\delta = \alpha$ differ in the first row, then $\gamma = \delta = \alpha$ and the cell is filled with a 1.

Construction 3.16 *([30]).* Let $\mathsf{O} = (\emptyset = \mu^0, \mu^1, \ldots, \mu^n = \emptyset)$ be an oscillating tableau. The associated triangular growth diagram is the Ferrers shape $(n-1, n-2, \ldots, 2, 1, 0)$. Label the cells according to the following specification:

(1) Label the north-east corners of the cells on the main diagonal from the top-left to the bottom-right with the partitions in O.
(2) For each $i \in \{0, \ldots, n-1\}$ label the corner on the first subdiagonal adjacent to the labels μ^i and μ^{i+1} with the partition $\mu^i \cap \mu^{i+1}$.
(3) Use the backwards rules B1-B6 to obtain all other labels and the fillings of the cells.

We denote by $\mathsf{G}_O(\mathsf{O})$ the symmetric $n \times n$ matrix one obtains from the filling of the growth diagram by putting zeros in the unfilled cells and along the diagonal and completing this to a symmetric matrix.

Starting from a filling of a growth diagram one obtains the oscillating tableau by setting all vectors on corners on the bottom and left border of the diagram to be the empty partition and applying the forwards growth rules F1-F6.

Next, we will extend these local rules to any filling of a Ferrers shape with non-negative integers.

3.3. Fomin growth diagrams: rule Burge

Given a filling of a Ferrers shape $(\lambda_1, \ldots, \lambda_\ell)$ with non-negative integers, we produce a "blow up" construction of the original shape for the Burge variant which contains south-east chains of 1's, as done by [21]. We begin by separating entries. If a cell is filled with a positive entry m, we replace the cell with an $m \times m$ grid of cells with 1's along the diagonal (from top-left to bottom-right). If there exist several nonzero entries in one column, we arrange the grids of cells also from top-left to bottom-right, so that the 1's form a south-east chain in each column. We make the same arrangements for the rows, also establishing a south-east chain in each row. The resulting blow up Ferrers diagram then contains c_j columns in the original j-th column, where c_j is equal to the sum of the entries in column j or 1 if the j-th column contains only 0's, and r_i rows in the original i-th row, where r_i is equal to the sum of the entries in row i or 1 if the i-th row contains only 0's. See Fig. 10.

Since the filling of the blow up growth diagram consists of 1's and 0's, we now apply the forward local rules. To start, we label all of the corners of the cells on the left side and the bottom side of the blow up growth diagram by $\emptyset$. Then we apply the forward local rules to determine the partition labels of the other corners, using the 0/1 filling and partitions defined in previous iterations of the forward local rule. Finally, we "shrink

Please cite this article in press as: J. Pappe et al., Promotion and growth diagrams for fans of Dyck paths and vacillating tableaux, J. Algebra (2023), https://doi.org/10.1016/j.jalgebra.2023.07.038

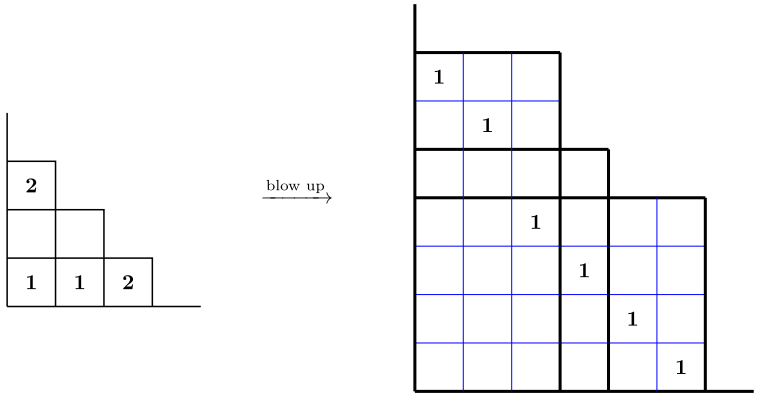

Fig. 10. An example of the blow up construction for Burge rules replacing positive integer entries with south-east chains of 1's in each column and row. (For interpretation of the colors in the figure(s), the reader is referred to the web version of this article.)

back" the labeled blow up growth diagram to obtain a labeling of the original Ferrers diagram by only considering the partitions labeling positions $\{(c_1+\cdots+c_j, r_i+\cdots+r_\ell) \mid 1 \leqslant i \leqslant \ell, 1 \leqslant j \leqslant \lambda_{\ell-i+1}\}$. These positions are precisely the intersections of the bolded black lines in Fig. 10. To shrink back, we ignore the labels on intersections involving any blue (or not bold) lines in the blow up growth diagram and assign the partition labeling $(c_1 + \cdots + c_j, r_i + \cdots + r_\ell)$ to the position $(j, \ell - i + 1)$ in the original Ferrers diagram. The resulting labeling has the property that partitions on adjacent corners differ by a vertical strip [21, Theorem 11].

We now describe the direct Burge forward and backwards rules [21, Section 4.4]. Consider a cell filled by a non-negative integer m, and labeled by the partitions γ, δ, α, where $\gamma \subset \delta$ and $\gamma \subset \alpha$, α/γ and δ/γ are vertical strips. Moreover, denote by $\mathbb{1}_A$ the truth function

$$\mathbb{1}_A = \begin{cases} 1 & \text{if } A \text{ is true,} \\ 0 & \text{otherwise.} \end{cases}$$

Then β is determined by the following procedure:

Burge F0: Set CARRY $:= m$ and $i := 1$.
Burge F1: Set $\beta_i := \max\{\delta_i, \alpha_i\} + \min\{\mathbb{1}_{\gamma_i=\delta_i=\alpha_i}, \text{CARRY}\}$
Burge F2: If $\beta_i = 0$, then stop and return $\beta = (\beta_1, \beta_2, \ldots, \beta_{i-1})$. If not, then set CARRY $:=$ CARRY $- \min\{\mathbb{1}_{\gamma_i=\delta_i=\alpha_i}, \text{CARRY}\} + \min\{\delta_i, \alpha_i\} - \gamma_i$ and $i := i+1$ and go to F1.

Note that this algorithm is reversible. Given β, δ, α such that β/δ and β/α are vertical strips, the backwards algorithm is defined by the following rules:

Burge B0: Set $i := \max\{j \mid \beta_j \text{ is positive}\}$ and CARRY $:= 0$.

Please cite this article in press as: J. Pappe et al., Promotion and growth diagrams for fans of Dyck paths and vacillating tableaux, J. Algebra (2023), https://doi.org/10.1016/j.jalgebra.2023.07.038

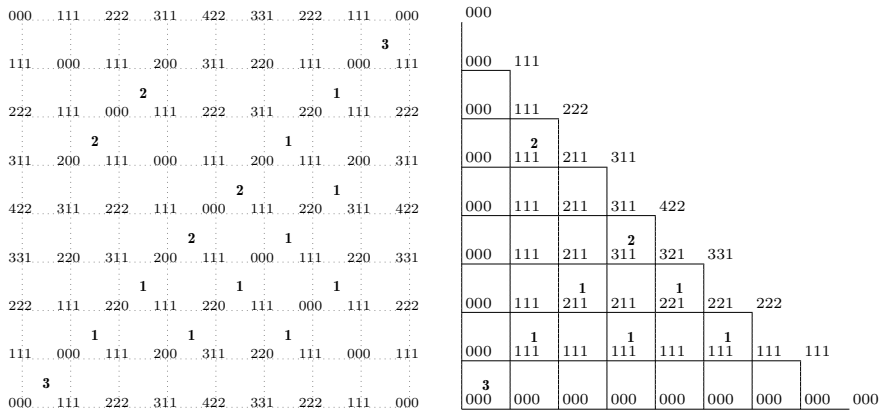

Fig. 11. On the left the filled promotion matrix of $\mathsf{F} = (000, 111, 222, 311, 422, 331, 222, 111, 000)$. On the right the triangular growth diagram for the same fan.

Burge B1: Set $\gamma_i := \min\{\delta_i, \alpha_i\} - \min\{\mathbb{1}_{\gamma_i=\alpha_i=\beta_i}, \mathrm{CARRY}\}$.

Burge B2: Set $\mathrm{CARRY} := \mathrm{CARRY} - \min\{\mathbb{1}_{\beta_i=\delta_i=\alpha_i}, \mathrm{CARRY}\} + \beta_i - \max\{\delta_i, \alpha_i\}$ and $i := i - 1$. If $i = 0$, then stop and return $\gamma = (\gamma_1, \gamma_2, \dots)$ and $m = \mathrm{CARRY}$. If not, got to B1.

Construction 3.17. Let $\mathsf{F} = (\emptyset = \mu^0, \mu^1, \dots, \mu^n = \emptyset)$ be an r-fan of Dyck paths. The associated triangular growth diagram is the Ferrers shape $(n-1, n-2, \dots, 2, 1, 0)$. Label the cells according to the following specification:

(1) Label the north-east corners of the cells on the main diagonal from the top-left to the bottom-right with the partitions in F.
(2) For each $i \in \{0, \dots, n-1\}$ label the corner on the first subdiagonal adjacent to the labels μ^i and μ^{i+1} with the partition $\mu^i \cap \mu^{i+1}$.
(3) Use the backwards rules Burge B0, B1 and B2 to obtain all other labels and the fillings of the cells.

We denote by $\mathsf{G}_F(\mathsf{F})$ the symmetric $n \times n$ matrix one obtains from the filling of the growth diagram by putting zeros in the unfilled cells and along the diagonal and completing this to a symmetric matrix.

Starting from a filling of a growth diagram one obtains the r-fan by filling the cells of a growth diagram, setting all vectors on corners on the bottom and left border of the diagram to be the empty partition and applying the forwards growth rules Burge F0-F2.

An example is given in Fig. 11.

3.4. Fomin growth diagrams: rule RSK

Given a filling of a Ferrers shape $(\lambda_1, \dots, \lambda_\ell)$ with non-negative integers, we produce a "blow up" construction of the original shape for the RSK variant which contains north-

Please cite this article in press as: J. Pappe et al., Promotion and growth diagrams for fans of Dyck paths and vacillating tableaux, J. Algebra (2023), https://doi.org/10.1016/j.jalgebra.2023.07.038

east chains of 1's, as done by [21]. We begin by separating entries. If a cell is filled with positive entry m, we replace the cell with an $m \times m$ grid of cells with 1's along the off-diagonal (from bottom-left to top-right). If there exist several nonzero entries in one column, we arrange the grids of cells also from bottom-left to top-right, so that the 1's form a north-east chain in each column. We make the same arrangements for the rows, also establishing a north-east chain in each row. The resulting blow up Ferrers diagram then contains c_j columns in the original j-th column, where c_j is equal to the sum of the entries in column j or 1 if the j-th column contains only 0's, and r_i rows in the original i-th row, where r_i is equal to the sum of the entries in row i or 1 if the i-th row contains only 0's.

Since the filling of the blow up growth diagram consists of 1's and 0's, we now apply the forward local rules. To start, we label all of the corners of the cells on the left side and the bottom side of the blow up growth diagram by $\emptyset$. Then, we apply the forward local rules to determine the partition labels of the other corners, using the 0/1 filling and partitions defined in previous iterations of the forward local rule. Finally, we "shrink back" the labeled blow up growth diagram to obtain a labeling of the original Ferrers diagram by only partitions labeling positions $\{(c_1+\cdots+c_j, r_i+\cdots+r_\ell) \mid 1 \leqslant i \leqslant \ell, 1 \leqslant j \leqslant \lambda_{\ell-i+1}\}$. To shrink back, we assign the partition labeling $(c_1 + \cdots + c_j, r_i + \cdots + r_\ell)$ in the blow up growth diagram to the position $(j, \ell - i + 1)$ in the original Ferrers diagram. The resulting labeling has the property that partitions on adjacent corners differ by a horizontal strip [21, Theorem 7].

The direct RSK forward rules are as follows [21, Section 4.1]: Consider a cell as in Fig. 9 filled by a non-negative integer m, and labeled by the partitions γ, δ, α, where $\gamma \subset \delta$ and $\gamma \subset \alpha$, α/γ and δ/γ are horizontal strips. Then β is determined by the following procedure:

RSK F0: Set CARRY $:= m$ and $i := 1$.
RSK F1: Set $\beta_i := \max\{\delta_i, \alpha_i\} + \text{CARRY}$
RSK F2: If $\beta_i = 0$, then stop and return $\beta = (\beta_1, \beta_2, \ldots, \beta_{i-1})$. If not, then set CARRY $:= \min\{\delta_i, \alpha_i\} - \gamma_i$ and $i := i + 1$ and go to F1.

Note that this algorithm is reversible. Given β, δ, α such that β/δ and β/α are horizontal strips, the backwards algorithm is defined by the following rules:

RSK B0: Set $i := \max\{j \mid \beta_j \text{ is positive}\}$ and CARRY $:= 0$.
RSK B1: Set $\gamma_i := \min\{\delta_i, \alpha_i\} - \text{CARRY}$.
RSK B2: Set CARRY $:= \beta_i - \max\{\delta_i, \alpha_i\}$ and $i := i - 1$. If $i = 0$, then stop and return $\gamma = (\gamma_1, \gamma_2, \ldots)$ and $m =$ CARRY. If not, got to B1.

Construction 3.18. Let $\mathsf{V} = (\emptyset = \mu^0, \mu^1, \ldots, \mu^n = \emptyset)$ be a vacillating tableau of weight zero. The associated triangular growth diagram is the Ferrers shape $(n-1, n-2, \ldots, 2, 1, 0)$. Label the cells according to the following specification:

Please cite this article in press as: J. Pappe et al., Promotion and growth diagrams for fans of Dyck paths and vacillating tableaux, J. Algebra (2023), https://doi.org/10.1016/j.jalgebra.2023.07.038

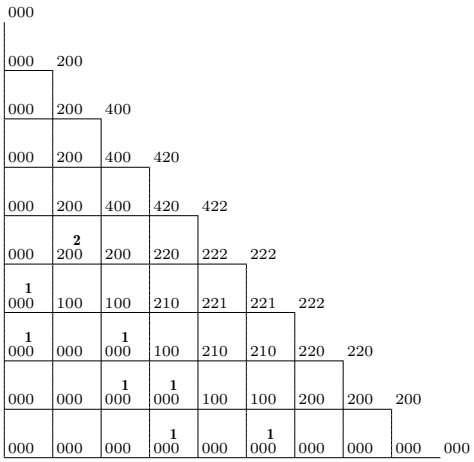

Fig. 12. The triangular growth diagram for the vacillating tableau $\mathsf{V} = (000, 100, 200, 210, 211, 111, 111, 110, 100, 000)$.

(1) Label the north-east corners of the cells on the main diagonal from the top-left to the bottom-right with the partitions $2\mu^i$.
(2) For each $i \in \{0, \dots, n-1\}$ label the corner on the first subdiagonal adjacent to the labels $2\mu^i$ and $2\mu^{i+1}$ with the partition $2(\mu^i \cap \mu^{i+1})$ when $\mu^i \neq \mu^{i+1}$ and the partition obtained by removing a cell from the final row of $2\mu^i$ when $\mu^i = \mu^{i+1}$.
(3) Use the backwards rules RSK B0, B1 and B2 to obtain all other labels and the fillings of the cells.

We denote by $\mathsf{G}_V(\mathsf{V})$ the symmetric $n \times n$ matrix one obtains from the filling of the growth diagram by putting zeros in the unfilled cells and along the diagonal and completing this to a symmetric matrix.

Starting from a filling of a growth diagram one obtains the vacillating tableau by setting all vectors on corners on the bottom and left border of the diagram to be the empty partition and applying the forwards growth rules RSK F0-F2.

The triangular growth diagram of the vacillating tableau from Example 3.11 is depicted in Fig. 12.

4. Main results

In this section, we state and prove our main results for oscillating tableaux, fans of Dyck paths, and vacillating tableaux. In particular, we show in Theorems 4.4, 4.5 and 4.11 that the fillings of the growth diagrams coincide with the fillings of the promotion–evacuation diagrams. This in turn shows that the maps M_F, $\mathsf{M}_{V\to O}$ and $\mathsf{M}_{V\to F}$ are injective. Having these injective maps to chord diagrams gives a first step towards a diagrammatic basis for the invariant subspaces. In Section 4.4, we give various new cyclic sieving phenomena associate to the promotion action.

Please cite this article in press as: J. Pappe et al., Promotion and growth diagrams for fans of Dyck paths and vacillating tableaux, J. Algebra (2023), https://doi.org/10.1016/j.jalgebra.2023.07.038

We begin by defining the following notation used later in this section. Let $M = (a_{i,j})_{i,j=1}^{kn}$ be a $kn \times kn$ matrix. It will often be convenient to consider M as the block matrix $(B_{i,j}^{(k)})_{i,j=1}^{n}$, where $B_{i,j}^{(k)}$ is the $k \times k$ matrix given by $(a_{p,q})_{p=k(i-1)+1,q=k(j-1)+1}^{ki,kj}$. We also follow the convention that for all $p, q > n$ we have $B_{p,q}^{(k)} := B_{i,j}^{(k)}$, where $p \equiv i \mod n$ and $q \equiv j \mod n$.

Definition 4.1. For a $kn \times kn$ matrix M with block matrix decomposition given by $(B_{i,j}^{(k)})_{i,j=1}^{n}$, denote by $\mathsf{blocksum}_k(M)$ the $n \times n$ matrix $(b_{i,j})_{i,j=1}^{n}$, where $b_{i,j}$ is equal to the sum of all entries in $B_{i,j}^{(k)}$.

Given an $n \times n$ matrix $M = (a_{i,j})_{i,j=1}^{n}$, we recursively define its skewed partial row sums $r_{i,j}$ by setting $r_{i,i} = 0$ for all $1 \leqslant i \leqslant n$ and letting $r_{i,j+1} = r_{i,j} + a_{i,j}$ for $1 \leqslant j \leqslant n-1$. Note that as before, we use the convention that $a_{p,q} = a_{i,j}$ whenever $p \equiv i \mod n$ and $q \equiv j \mod n$. Similarly, the skewed partial column sums $c_{i,j}$ can be defined. Partial inverses to $\mathsf{blocksum}_k$ are given by $\mathsf{blowup}_k^{\mathsf{SE}}$ and $\mathsf{blowup}_k^{\mathsf{NE}}$ which we presently define.

Definition 4.2. Let $M = (a_{i,j})_{i,j=1}^{n}$ be a matrix with non-negative integer entries such that for each row and for each column the sum of the entries is k. Let $r_{i,j}$ and $c_{i,j}$ be its skewed partial row and column sums respectively. Let $B_{i,j}^{SE}$ be the $k \times k$ matrix, where $B_{i,j}^{SE}$ is the zero-matrix if $a_{i,j} = 0$ and a zero-one-matrix if $a_{i,j} \neq 0$ consisting of 1's in positions $(r_{i,j}+1, c_{i,j}+1), \ldots, (r_{i,j}+a_{i,j}, c_{i,j}+a_{i,j})$ and zeros elsewhere. We define $\mathsf{blowup}^{\mathsf{SE}}(M)$ to be the block matrix $(B_{i,j}^{SE})_{i,j=1}^{n}$.

Similarly, let $B_{i,j}^{NE}$ be the $k \times k$ matrix, where $B_{i,j}^{BE}$ is the zero-matrix if $a_{i,j} = 0$ and a zero-one-matrix if $a_{i,j} \neq 0$ consisting of 1's in positions $(k - r_{i,j}, k - c_{i,j} - a_{i,j} + 1), \ldots, (k - r_{i,j} - (a_{i,j} - 1), k - c_{i,j})$ and zeros elsewhere. We define $\mathsf{blowup}^{\mathsf{NE}}(M)$ to be the block matrix $(B_{i,j}^{NE})_{i,j=1}^{n}$.

Remark 4.3. Note that $\mathsf{blowup}^{\mathsf{SE}}(M)$ and $\mathsf{blowup}^{\mathsf{NE}}(M)$ are the unique $kn \times kn$ zero-one-matrices whose $\mathsf{blocksum}_k$ equals M and for all $1 \leqslant i \leqslant n$, the nonzero entries in the matrices

$$[B_{i,i}, B_{i,i+1}, B_{i,i+2}, \ldots, B_{i,i+n-1}] \qquad \text{and}$$
$$[B_{i,i}, B_{i+1,i}, B_{i+2,i}, \ldots, B_{i+n-1,i}]$$

form a south-east chain or a north-east chain, respectively.

4.1. Results for oscillating tableaux

The next result was not stated explicitly in [30], but can be deduced from the proof in the paper.

Please cite this article in press as: J. Pappe et al., Promotion and growth diagrams for fans of Dyck paths and vacillating tableaux, J. Algebra (2023), https://doi.org/10.1016/j.jalgebra.2023.07.038

Theorem 4.4. *For an oscillating tableau of weight zero* O *the fillings of the growth diagram (Construction 3.16) and the fillings of the promotion-evacuation (Construction 3.3) diagram coincide, that is*

$$\mathsf{G}_O(\mathsf{O}) = \mathsf{M}_O(\mathsf{O}).$$

Proof. This follows from the proof of [30, Corollary 6.17, Lemma 6.26]. □

4.2. Results for r-fans of Dyck paths

We state our main results.

Theorem 4.5. *For an* r*-fan of Dyck paths* F

$$\mathsf{G}_F(\mathsf{F}) = \mathsf{M}_F(\mathsf{F}).$$

In other words, the fillings of its growths diagram (Construction 3.17) and the fillings of the promotion-evacuation diagram coincide.

In particular we obtain the corollary:

Corollary 4.6. *The map* M_F *is injective.*

We now state and prove some results which are needed for the proof of Theorem 4.5.

Lemma 4.7. *Let* F *be an* r*-fan of Dyck paths of length* n*. Then*

$$\iota_{F\to O} \circ \mathsf{pr}_{\mathcal{B}_{\mathsf{spin}}}(\mathsf{F}) = \mathsf{pr}^r_{\mathcal{C}_\square} \circ \iota_{F\to O}(\mathsf{F}).$$

Proof. Let $\iota_{F\to O}(\mathsf{F}) = \mu = (\emptyset = \mu^{(0,0)}, \dots, \mu^{(0,rn)} = \emptyset)$. We first prove that $\mathsf{pr}^r_{\mathcal{C}_\square}(\mu) = \mathsf{pr}_{\mathcal{C}^{\otimes r}_\square}(\mu)$. Let $\mathsf{pr}^i_{\mathcal{C}_\square}(\mu) = (\emptyset = \mu^{(i,0)}, \dots, \mu^{(i,rn)} = \emptyset)$. From the definition of $\iota_{F\to O}$, we have $\mu^{(0,k)} = (1^k)$ for all $0 \leqslant k \leqslant r$ where (1^0) denotes the empty partition $\emptyset$. Using the local rules for promotion and induction, we see that the sequence of partitions $(\mu^{(k,0)}, \dots, \mu^{(k,r-k)})$ is equal to $((1^0), \dots, (1^{r-k}))$ for all $0 \leqslant k \leqslant r$. This implies the following equality

$$\begin{aligned}\mu &= ((1^0), (1^1), \dots, (1^r), \mu^{(0,r+1)}, \dots, \mu^{(0,rn)}) \\ &= (\mu^{(r,0)}, \mu^{(r-1,1)}, \dots, \mu^{(0,r)}, \mu^{(0,r+1)}, \dots, \mu^{(0,rn)}).\end{aligned}$$

By a similar argument, the sequence of partitions $(\mu^{(k,rn-k)}, \dots, \mu^{(k,rn)})$ is equal to $((1^k), \dots, (1^0))$ for all $1 \leqslant k \leqslant r$ implying

Please cite this article in press as: J. Pappe et al., Promotion and growth diagrams for fans of Dyck paths and vacillating tableaux, J. Algebra (2023), https://doi.org/10.1016/j.jalgebra.2023.07.038

$$\begin{aligned}\mathsf{pr}^r_{\mathcal{C}^{\otimes}_{\square}}(\mu) &= (\mu^{(r,0)}, \mu^{(r,1)}, \dots, \mu^{(r,r(n-1)-1)}, (1^r), (1^r - 1), \dots, (1^0)) \\ &= (\mu^{(r,0)}, \mu^{(r,1)}, \dots, \mu^{(r,rn-r-1)}, \mu^{(r,rn-r)}, \mu^{(r-1,rn-r-1)}, \dots, \mu^{(0,r)}).\end{aligned}$$

By Theorem 2.27, we obtain the desired equality

$$\begin{aligned}\mathsf{pr}_{\mathcal{C}^{\otimes r}_{\square}}(\mu) &= \mathsf{pr}_{\mathcal{C}^{\otimes r}_{\square}}(\mu^{(r,0)}, \mu^{(r-1,1)}, \dots, \mu^{(0,r)}, \mu^{(0,r+1)}, \dots, \mu^{(0,rn)}) \\ &= (\mu^{(r,0)}, \mu^{(r,1)}, \dots, \mu^{(r,r(n-1))}, \mu^{(r-1,r(n-1)+1)}, \dots, \mu^{(0,rn)}) = \mathsf{pr}^r_{\mathcal{C}_{\square}}(\mu).\end{aligned}$$

Let $w = w_n \otimes w_{n-1} \otimes \cdots \otimes w_1 \in \mathcal{B}^{\otimes n}_{\mathsf{spin}}$ and $v = v_{rn} \otimes v_{rn-1} \otimes \cdots \otimes v_1 \in (\mathcal{C}^{\otimes r}_{\square})^{\otimes n}$ be the highest weight crystal elements associated to F and μ, respectively. In order to show $\iota_{F\to O} \circ \mathsf{pr}_{\mathcal{B}_{\mathsf{spin}}}(\mathsf{F}) = \mathsf{pr}_{\mathcal{C}^{\otimes r}_{\square}}(\mu)$, it suffices to show that $\Psi(\mathsf{pr}_{\mathcal{B}_{\mathsf{spin}}}(w)) = \mathsf{pr}_{\mathcal{C}^{\otimes r}_{\square}}(v)$, where Ψ is the crystal isomorphism defined in Definition 2.7. Let $\mathcal{V} \subseteq \mathcal{C}^{\otimes r}_{\square}$ be the virtual crystal defined in Definition 2.4. As Ψ is a crystal isomorphism, we have $\Psi(\mathsf{pr}_{\mathcal{B}_{\mathsf{spin}}}(w)) = \mathsf{pr}_{\mathcal{V}}(\Psi(w)) = \mathsf{pr}_{\mathcal{V}}(v)$. As Lusztig's involution for crystals of type B_r and C_r interchanges the crystal operators f_i and e_i, the virtualization induced by the embedding $B_r \hookrightarrow C_r$ commutes with Lusztig's involution. In addition virtualization is preserved under tensor products (see for example [3, Theorem 5.8]). Thus, we have $\mathsf{pr}_{\mathcal{V}}(v) = \mathsf{pr}_{\mathcal{C}^{\otimes r}_{\square}}(v)$. □

Lemma 4.8. *Let F be an r-fan of Dyck paths with length n, and let $(B^{(r)}_{i,j})^n_{i,j=1}$ be the block matrix decomposition of the $rn \times rn$ adjacency matrix $\mathsf{M}_O(\iota_{F\to O}\mathsf{F})$. Then for all $1 \leqslant i \leqslant n$, the nonzero entries in the matrices*

$$[B^{(r)}_{i,i+1}, B^{(r)}_{i,i+2}, \dots, B^{(r)}_{i,i+n-1}] \qquad \textit{and}$$
$$[B^{(r)}_{i+1,i}, B^{(r)}_{i+2,i}, \dots, B^{(r)}_{i+n-1,i}]$$

form a south-east chain of r 1's.

Proof. By the definition of oscillating tableaux and the local rules for promotion, M_O is a zero-one matrix. From Lemma 4.7, Proposition 3.2, and Proposition 3.13, it suffices to prove that the nonzero entries in $[B^{(r)}_{n,n+1}, B^{(r)}_{n,n+2}, \dots, B^{(r)}_{n,2n-1}]$ and $[B^{(r)}_{2,1}, B^{(r)}_{3,1}, \dots, B^{(r)}_{n,1}]^T$ form a south-east chain. Recall that by construction, the Fomin growth diagram of $\iota_{F\to O}(\mathsf{F})$ is a triangle diagram with the entries of $\iota_{F\to O}(\mathsf{F})$ labeling its diagonal. As F is an r-fan of Dyck paths, the partition (1^r) sits at the corners $(r, r(n-1))$ and $(r(n-1), r)$ in the Fomin growth diagram of $\iota_{F\to O}(\mathsf{F})$. By Theorem 4.4, we have $\mathsf{M}_O(\iota_{F\to O}(\mathsf{F})) = \mathsf{G}_O(\iota_{F\to O}(\mathsf{F}))$. This implies that the filling of the leftmost r columns and bottommost r rows matches $\mathsf{M}_O(\iota_{F\to O}(\mathsf{F}))$. As all the entries of $\mathsf{M}_O(\iota_{F\to O}(\mathsf{F}))$ are either 0 or 1, we have by [21, Theorem 2] that there are exactly r 1's forming a south-east chain in the leftmost r columns and in the bottommost r rows. □

Remark 4.9. The proof of Lemma 4.8 implies that the diagonal block matrices $B^{(r)}_{i,i}$ of $\mathsf{M}_O(\iota_{F\to O}\mathsf{F})$ are all zero matrices.

Please cite this article in press as: J. Pappe et al., Promotion and growth diagrams for fans of Dyck paths and vacillating tableaux, J. Algebra (2023), https://doi.org/10.1016/j.jalgebra.2023.07.038

Proposition 4.10. *Let* F *be an* r*-fan of Dyck paths of length* n*. Then*

$$\mathsf{M}_F(\mathsf{F}) = \mathsf{blocksum}_r(\mathsf{M}_O(\iota_{F\to O}(\mathsf{F}))).$$

Moreover,

$$\mathsf{blowup}_r^{\mathsf{SE}}(\mathsf{M}_F(\mathcal{F})) = \mathsf{M}_O(\iota_{F\to O}(\mathcal{F})).$$

Proof. By Remark 4.9, the diagonal entries of $\mathsf{M}_F(\mathsf{F})$ and $\mathsf{blocksum}_r(\mathsf{M}_O(\iota_{F\to O}(\mathsf{F})))$ are all zero. Let $a_{i,j}$ with $i \neq j$ be the entry in $\mathsf{M}_F(\mathsf{F})$ that is the filling of the cell labeled by

$\begin{array}{|c|c} \lambda & \nu \\ \hline \kappa & \end{array}\ \mu$ in the promotion matrix of F. To show that the number of 1's appearing in $B_{i,j}^{(r)}$ of $\mathsf{M}_O(\iota_{F\to O}(\mathsf{F}))$ is also equal to $a_{i,j}$, we first compute $a_{i,j}$ for $i \neq j$. By Definition (3.3), $a_{i,j}$ is the number of negative entries in $\kappa + \nu - \lambda$. Since λ, ν and κ, μ are consecutive partitions in an r-fan of Dyck paths, we know that they differ by a vector of the form $(\pm 1, \ldots, \pm 1)$. We may write $\nu - \lambda$ and $\mu - \kappa$ as

$$\begin{aligned} \nu - \lambda &= \mathbf{e}_{i_1} + \cdots + \mathbf{e}_{i_k} - \mathbf{e}_{i_{k+1}} - \cdots - \mathbf{e}_{i_r}, \\ \mu - \kappa &= \mathbf{e}_{j_1} + \cdots + \mathbf{e}_{j_m} - \mathbf{e}_{j_{m+1}} - \cdots - \mathbf{e}_{j_r}, \end{aligned}$$

where

$$\begin{aligned} &\{i_1, \ldots, i_r\} = [r] = \{j_1, \ldots, j_r\}, \\ &i_1 < \cdots < i_k \text{ and } i_{k+1} > \cdots > i_r, \\ &j_1 < \cdots < j_m \text{ and } j_{m+1} > \cdots > j_r. \end{aligned}$$

By the definition of μ from the local rules of Lenart [23] (see Section 2.5), we have

$$\begin{aligned} \mu &= \mathrm{dom}_{\mathfrak{H}_r}(\kappa + \nu - \lambda) \\ &= \mathrm{dom}_{\mathfrak{H}_r}(\kappa + \mathbf{e}_{i_1} + \cdots + \mathbf{e}_{i_k} - \mathbf{e}_{i_{k+1}} - \cdots - \mathbf{e}_{i_r}). \end{aligned}$$

Recall that $\mathrm{dom}_{\mathfrak{H}_r}$ applied to a weight sorts the absolute values of the entries of the weight into weakly decreasing order. In particular, $\mathrm{dom}_{\mathfrak{H}_r}(\kappa + \mathbf{e}_{i_1} + \cdots + \mathbf{e}_{i_k} - \mathbf{e}_{i_{k+1}} - \cdots - \mathbf{e}_{i_r})$ will change all of the -1 entries of $\kappa + \mathbf{e}_{i_1} + \cdots + \mathbf{e}_{i_k} - \mathbf{e}_{i_{k+1}} - \cdots - \mathbf{e}_{i_r}$ to $+1$ and then sort all entries into weakly decreasing order (note that sorting will not change the number of cells). We thus have two equations for μ:

$$\begin{aligned} \mu &= \mathrm{dom}_{\mathfrak{H}_r}(\kappa + \mathbf{e}_{i_1} + \cdots + \mathbf{e}_{i_k} - \mathbf{e}_{i_{k+1}} - \cdots - \mathbf{e}_{i_r}) \\ &= \kappa + \mathbf{e}_{j_1} + \cdots + \mathbf{e}_{j_m} - \mathbf{e}_{j_{m+1}} - \cdots - \mathbf{e}_{j_r}. \end{aligned}$$

Therefore, $\mathrm{dom}_{\mathfrak{H}_r}$ changed $m - k$ negative entries in $\kappa + \nu - \lambda$ to $+1$ in μ, showing that $a_{i,j} = m - k$.

Please cite this article in press as: J. Pappe et al., Promotion and growth diagrams for fans of Dyck paths and vacillating tableaux, J. Algebra (2023), https://doi.org/10.1016/j.jalgebra.2023.07.038

From the virtualization given in Definition 2.7, the partitions labeling the top of the first row of cells in $B^{(r)}_{i,j}$ are $\lambda, \lambda^{(1)}, \ldots, \lambda^{(r-1)}, \nu$, where $\lambda^{(\ell)} = \lambda + \mathbf{e}_{i_1} + \cdots \pm \mathbf{e}_{i_\ell}$. Similarly, the partitions labeling the bottom of the r-th row of cells in $B^{(r)}_{i,j}$ are $\kappa, \kappa^{(1)}, \ldots, \kappa^{(r-1)}, \mu$, where $\kappa^{(\ell)} = \kappa + \mathbf{e}_{j_1} + \cdots \pm \mathbf{e}_{j_\ell}$. In particular, we have

$$\lambda \subset \lambda^{(1)} \subset \cdots \subset \lambda^{(k-1)} \subset \lambda^{(k)} \supset \lambda^{(k+1)} \supset \cdots \supset \lambda^{(r-1)} \supset \nu,$$
$$\kappa \subset \kappa^{(1)} \subset \cdots \subset \kappa^{(m-1)} \subset \kappa^{(m)} \supset \kappa^{(m+1)} \supset \cdots \supset \kappa^{(r-1)} \supset \mu.$$

Let $\begin{array}{cc} \lambda' & \nu' \\ \boxed{\kappa'} & \mu' \end{array}$ label a cell in the first row of $B^{(r)}_{i,j}$, and note that the pairs λ', ν' and κ', μ' differ by a unit vector since they are adjacent partitions in an oscillating tableau.

It is impossible for the inclusions $\begin{array}{c} \lambda' \subset \nu' \\ \boxed{\kappa'} \supset \mu' \end{array}$ since $\lambda' \subset \nu'$ implies $\kappa' + \nu' - \lambda' = \kappa' + \mathbf{e}_i$ for some i, and by definition $\mu' = \mathrm{dom}_{\mathfrak{H}_r}(\kappa' + \mathbf{e}_i) = \kappa' + \mathbf{e}_i$ which contradicts $\mu' \subset \kappa'$.

When $\begin{array}{c} \lambda' \supset \nu' \\ \boxed{\kappa'} \subset \mu' \end{array}$ occurs, we know that $\kappa' + \nu' - \lambda' = \kappa' - \mathbf{e}_i$ for some i since $\nu' \subset \lambda'$. Since $\kappa' \subset \mu' = \mathrm{dom}_{\mathfrak{H}_r}(\kappa' - \mathbf{e}_i)$, it must be that $\mu' = \kappa' + \mathbf{e}_i$ and therefore $\kappa' - \mathbf{e}_i$ contained a negative entry. Therefore, when $\lambda' \supset \nu'$ and $\kappa' \subset \mu'$ there is a 1 filling the cell. Conversely, when there is a 1 filling a cell labeled $\begin{array}{cc} \lambda' & \nu' \\ \boxed{\kappa'} & \mu' \end{array}$, then there is a negative in $\kappa' + \nu' - \lambda' = \kappa' \pm \mathbf{e}_i$ for some i, which is only possible when $\kappa' + \nu' - \lambda' = \kappa' - \mathbf{e}_i$. As a result, $\kappa' \subset \mu'$ and $\lambda' \supset \nu'$.

By Theorem 4.4, each row and each column in $\mathsf{M}_O(\iota_{F\to O}(\mathsf{F}))$ contains exactly one 1. Therefore there is at most one cell in the first row of $B^{(r)}_{i,j}$ where the containment between the top and bottom pairs of partitions is flipped. By the cases described above, containment between pairs of partitions labeling the bottom of the first row of cells in $B^{(r)}_{i,j}$ either exactly matches the containment between pairs of partitions labeling the top of the first row or the switch in containment in the bottom occurs immediately to the right of the switch in containment in the top. The same outcome is observed recursively in the remaining rows of cells in $B^{(r)}_{i,j}$. Since we already knew the labels of the bottom of the r-th row to be increasing up to $\kappa^{(m)}$, we conclude that the number of 1's appearing in $B^{(r)}_{i,j}$ is equal to $m - k$, which we showed above is equal to $a_{i,j}$. Therefore, $\mathsf{M}_F(\mathsf{F}) = \mathsf{blocksum}_r(\mathsf{M}_O(\iota_{F\to O}(\mathsf{F})))$. Further, since the 1's in $\mathsf{M}_O(\iota_{F\to O}(\mathsf{F}))$ form a south-east chain, by Remark 4.3 we have $\mathsf{blowup}^{\mathsf{SE}}_r(\mathsf{M}_F(\mathsf{F})) = \mathsf{M}_O(\iota_{F\to O}(\mathsf{F}))$. □

We can now prove Theorem 4.5.

Please cite this article in press as: J. Pappe et al., Promotion and growth diagrams for fans of Dyck paths and vacillating tableaux, J. Algebra (2023), https://doi.org/10.1016/j.jalgebra.2023.07.038

Proof. Let $\mathsf{F} = (\mu^0, \ldots, \mu^n)$ be an r-fan of Dyck paths of length n. We have

$$\begin{aligned} \mathsf{M}_F(\mathsf{F}) &= \mathsf{blocksum}_r(\mathsf{M}_O(\iota_{F\to O}(\mathsf{F}))) && \text{by Proposition 4.10} \\ &= \mathsf{blocksum}_r(\mathsf{G}_O(\iota_{F\to O}(\mathsf{F}))) && \text{by Theorem 4.4.} \end{aligned}$$

It remains to show that $\mathsf{blocksum}_r(\mathsf{G}_O(\iota_{F\to O}(\mathsf{F}))) = \mathsf{G}_F(\mathsf{F})$. The diagonal entries of $\mathsf{blocksum}_r(\mathsf{G}_O(\iota_{F\to O}(\mathsf{F})))$ and $\mathsf{G}_F(\mathsf{F})$ are all zero by Remark 4.9 and by definition of G_F respectively. As G_O and G_F are symmetric matrices, it suffices to show that the lower triangular entries of $\mathsf{blocksum}_r(\mathsf{G}_O(\iota_{F\to O}(\mathsf{F})))$ and $\mathsf{G}_F(\mathsf{F})$ agree. Let G denote the triangular growth diagram associated with $\iota_{F\to O}(\mathsf{F})$. By the definition of $\iota_{F\to O}$ and Construction 3.16, the coordinate $(kr, (n-k)r)$ is labeled with partition μ^k for $0 \leqslant k \leqslant n$. As G has a 0/1 filling, the local rules guarantee that the partition ν^k labeling the coordinate $(kr, (n-k-1)r)$ of G is contained within the partition $\mu^k \cap \mu^{k+1}$ for $0 \leqslant k \leqslant n-1$. Moreover, $|\mu^k/\nu^k| + |\mu^{k+1}/\nu^k|$ is equal to the total number of 1's lying in either a column from $kr+1$ to $(k+1)r$ or in a row from $(n-k-1)r+1$ to $(n-k)r$. From Lemma 4.8 and the fact that G_O is symmetric, there exist exactly r such 1's which implies $|\mu^k/\nu^k| + |\mu^{k+1}/\nu^k| = r$. Since μ^k and μ^{k+1} differ by exactly k boxes, $\nu^k = \mu^k \cap \mu^{k+1}$ for all $0 \leqslant k \leqslant n-1$.

Let H denote the triangular growth diagram with filling given by the lower triangular entries of $\mathsf{blocksum}_r(\mathsf{G}_O(\iota_{F\to O}(\mathsf{F})))$ and local rules given by the Burge rules. From Lemma 4.8, $\mathsf{blowup}^{\mathsf{SE}}(\mathsf{blocksum}_r(\mathsf{G}_O(\iota_{F\to O}(\mathsf{F})))) = \mathsf{G}_O(\iota_{F\to O}(\mathsf{F}))$. A result by Krattenthaler [21] implies that the labellings of the hypotenuse of H are given by $(\mu^0, \nu^0, \mu^1, \ldots, \nu^{n-1}, \mu^n)$. As the Burge rules are injective and the growth diagram associated to F under Construction 3.17 has hypotenuse labeled by $(\mu^0, \mu^0 \cap \mu^1, \mu^1, \ldots, \mu^{n-1} \cap \mu^n, \mu^n)$, the lower triangular entries of $\mathsf{blocksum}_r(\mathsf{G}_O(\iota_{F\to O}(\mathsf{F})))$ and $\mathsf{G}_F(\mathsf{F})$ are equal. □

4.3. Results for vacillating tableaux

We state our main results.

Theorem 4.11. *For a vacillating tableau* V

$$\mathsf{G}_V(\mathsf{V}) = \mathsf{M}_{V\to O}(\mathsf{V}) = \mathsf{M}_{V\to F}(\mathsf{V}).$$

In other words, the filling of the growth diagram (see Construction 3.18), the filling of the promotion matrix $\mathsf{M}_{V\to O}(\mathsf{V})$*, and the filling of the promotion matrix* $\mathsf{M}_{V\to F}(\mathsf{V})$ *coincide.*

In particular we obtain the corollary:

Corollary 4.12. *The maps* $\mathsf{M}_{V\to O}$ *and* $\mathsf{M}_{V\to F}$ *are injective.*

Please cite this article in press as: J. Pappe et al., Promotion and growth diagrams for fans of Dyck paths and vacillating tableaux, J. Algebra (2023), https://doi.org/10.1016/j.jalgebra.2023.07.038

We will first prove the second equality in Theorem 4.11. To do so, we need the following lemma.

Lemma 4.13. *We have the following:*

(i) $\mathsf{M}_{V\to O} = \mathsf{blocksum}_2 \circ \mathsf{M}_O \circ \iota_{V\to O}$.
(ii) *Denote by* E *the* $r \times r$ *identity matrix, then*

$$\mathsf{M}_{V\to F} + 2(r-1)E = \mathsf{blocksum}_2 \circ \mathsf{M}_F \circ \iota_{V\to F}.$$

Proof. Let V be a vacillating tableau of length n and weight zero and let $X \in \{O, F\}$. Denote by $\mathsf{T} = (\emptyset = \mu^0, \mu^1, \dots, \mu^{2n} = \emptyset)$ the corresponding oscillating tableau (resp. r-fan of Dyck path) to V using $\iota_{V\to X}$.

Recall that $\mathsf{M}_{V\to X}$ is defined using the Schema (3.5) to calculate promotion. Let $\hat{\hat{\mu}}^1, \dots, \hat{\hat{\mu}}^{2n-1}$ be the partitions in the middle row in of this schema.

Note that we have $\mu^2 = \hat{\mu}^{2n-2} = 2\mathbf{e}_1$ and

$$\mu^1 = \hat{\hat{\mu}}^1 = \hat{\hat{\mu}}^{2n-1} = \hat{\mu}^{2n-1} = \begin{cases} \mathbf{e}_1 & \text{if } X = O, \\ \mathbf{1} & \text{if } X = F. \end{cases}$$

It is easy to see that the squares

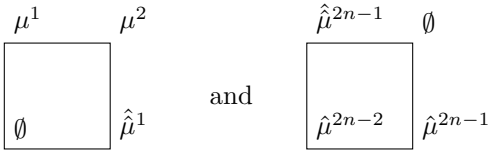

satisfy the local rule and

$$\Phi(\mu^1, \emptyset, \mu^2, \hat{\hat{\mu}}^1) = \Phi(\hat{\hat{\mu}}^{2n-1}, \hat{\mu}^{2n-2}, \emptyset, \hat{\mu}^{2n-1}) = \begin{cases} 0 & \text{if } X = O, \\ r-1 & \text{if } X = F. \end{cases}$$

Thus we have

$$\mathsf{pr}_X(\iota_{V\to X}(\mathsf{V})) = (\emptyset, \hat{\hat{\mu}}_1, \dots, \hat{\hat{\mu}}_{2n-1}, \emptyset)$$

and obtain $\mathsf{M}_{V\to X} + \mathbb{1}_{X=F} \cdot 2(r-1)E = \mathsf{blocksum}_2 \circ \mathsf{M}_X \circ \iota_{V\to X}$. □

The following relates the growth diagrams for $\iota_{V\to O}(\mathsf{V})$ and $\iota_{V\to F}(\mathsf{V})$.

Please cite this article in press as: J. Pappe et al., Promotion and growth diagrams for fans of Dyck paths and vacillating tableaux, J. Algebra (2023), https://doi.org/10.1016/j.jalgebra.2023.07.038

Lemma 4.14. *Denote by S the $2r \times 2r$ block diagonal matrix consisting of r copies of the block* $\begin{bmatrix} 0 & 1 \\ 1 & 0 \end{bmatrix}$ *along the diagonal and zeros everywhere else. Then*

$$\mathsf{G}_F \circ \iota_{V \to F} = \mathsf{G}_O \circ \iota_{V \to O} + (r-1)S.$$

Proof. Let $\mathsf{V} = (\lambda^0, \ldots, \lambda^n)$ be a vacillating tableau of weight zero. Denote with $\mathsf{O} = (\mu^0, \ldots, \mu^{2n}) = \iota_{V \to O}(\mathsf{V})$ the corresponding oscillating tableaux and denote with $\mathsf{F} = (\nu^0, \ldots, \nu^{2n}) = \iota_{V \to O}(F)$ the r-fan of Dyck paths.

Consider the portion of the growth diagram for the oscillating tableau involving only $(\mu^{2i-2}, \mu^{2i-1}, \mu^{2i})$ and the portion of the growth diagram for the fan of Dyck paths involving only $(\nu^{2i-2}, \nu^{2i-1}, \nu^{2i})$. We label the partitions as follows.

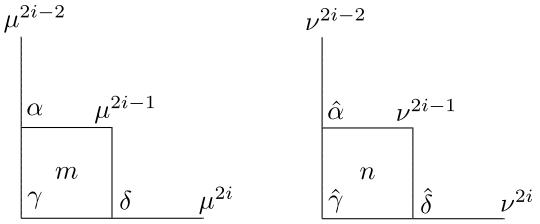

(4.1)

Claim. *We have $\mu^{2i-2} = \nu^{2i-2}$, $\mu^{2i} = \nu^{2i}$, $\alpha = \hat{\alpha}$, $\gamma = \hat{\gamma}$, $\delta = \hat{\delta}$, $m = 0$ and $n = r-1$. Moreover all partitions on consecutive corners on the lower left border of the diagrams in (4.1) differ by at most one cell.*

We consider the three cases $\lambda^{i-1} = \lambda^i$, $\lambda^{i-1} \subset \lambda^i$ and $\lambda^{i-1} \supset \lambda^i$.

By Definition 2.21, Construction 3.16, Definition 2.22 and Construction 3.17 we have

$$\begin{aligned} \mu^{2i-2} &= \nu^{2i-2} = 2\lambda^{i-1}, & \mu^{2i} &= \nu^{2i} = 2\lambda^i, \\ \alpha &= \mu^{2i-2} \cap \mu^{2i-1}, & \delta &= \mu^{2i-1} \cap \mu^{2i}, \\ \hat{\alpha} &= \nu^{2i-2} \cap \nu^{2i-1}, & \hat{\delta} &= \nu^{2i-1} \cap \nu^{2i}. \end{aligned}$$

Case I. Assume $\lambda^{i-1} = \lambda^i$. In this case we have $\mu^{2i-1} = 2\lambda^i - \mathbf{e}_r$ and $\nu^{2i-1} = 2\lambda^i + \mathbf{1} - 2\mathbf{e}_r$ and get

$$\begin{aligned} \alpha = \delta &= (2\lambda^i) \cap (2\lambda^i - \mathbf{e}_r) = 2\lambda^i - \mathbf{e}_r, \\ \hat{\alpha} = \hat{\delta} &= (2\lambda^i) \cap (2\lambda^i + \mathbf{1} - 2\mathbf{e}_r) = 2\lambda^i - \mathbf{e}_r. \end{aligned}$$

Using the backwards rules for growth diagrams we obtain

$$\gamma = \hat{\gamma} = 2\lambda^i - \mathbf{e}_r, \quad m = 0 \quad \text{and} \quad n = r-1.$$

Please cite this article in press as: J. Pappe et al., Promotion and growth diagrams for fans of Dyck paths and vacillating tableaux, J. Algebra (2023), https://doi.org/10.1016/j.jalgebra.2023.07.038

Case II. Assume $\lambda^{i-1} \subset \lambda^i$. In this case we have $\mu^{2i-1} = \lambda^{i-1} + \lambda^i$ and $\nu^{2i-1} = 2\lambda^{i-1} + \mathbf{1}$. Furthermore we obtain

$$\begin{aligned}
\alpha &= (2\lambda^{i-1}) \cap (\lambda^{i-1} + \lambda^i) = 2\lambda^{i-1}, \\
\hat{\alpha} &= (2\lambda^{i-1}) \cap (2\lambda^{i-1} + \mathbf{1}) = 2\lambda^{i-1}, \\
\delta &= (\lambda^{i-1} + \lambda^i) \cap (2\lambda^i) = \lambda^{i-1} + \lambda^i, \\
\hat{\delta} &= (2\lambda^{i-1} + \mathbf{1}) \cap (2\lambda^i) = \lambda^{i-1} + \lambda^i.
\end{aligned}$$

Using the backwards rules for growth diagrams we obtain

$$\gamma = \hat{\gamma} = 2\lambda^{i-1}, \quad m = 0 \quad \text{and} \quad n = r - 1.$$

Case III. Assume $\lambda^{i-1} \supset \lambda^i$. This case is symmetric to Case II.

This proves the claim.

The rest of the growth diagrams must agree, as the Burge growth rules and Fomin growth rules agree in the case where labels on consecutive corners differ by at most one cell. □

Note that Lemma 4.14 implies

$$\mathsf{blocksum}_2 \circ \mathsf{G}_F \circ \iota_{V \to F} = \mathsf{blocksum}_2 \circ \mathsf{G}_O \circ \iota_{V \to O} + 2(r-1)E. \tag{4.2}$$

Now we can prove the second identity of Theorem 4.11.

Proof. We have

$$\begin{aligned}
\mathsf{M}_{V \to O} &= \mathsf{blocksum}_2 \circ \mathsf{M}_O \circ \iota_{V \to O} && \text{by Lemma 4.13 (i)} \\
&= \mathsf{blocksum}_2 \circ \mathsf{G}_O \circ \iota_{V \to O} && \text{by Theorem 4.4} \\
&= \mathsf{blocksum}_2 \circ \mathsf{G}_F \circ \iota_{V \to F} - 2(r-1)E && \text{by Equation (4.2)} \\
&= \mathsf{blocksum}_2 \circ \mathsf{M}_F \circ \iota_{V \to F} - 2(r-1)E && \text{by Theorem 4.5} \\
&= \mathsf{M}_{V \to F} && \text{by Lemma 4.13 (ii).} \quad \square
\end{aligned}$$

It is possible to invert Lemma 4.13 (i) as follows.

Lemma 4.15. *Let* V *be a vacillating tableau of weight zero with length* n*, and let* $(B^{(2)}_{i,j})_{i,j=1}^n$ *be the block matrix decomposition of the* $2n \times 2n$ *adjacency matrix* $\mathsf{M}_O(\iota_{V \to O}\mathsf{V})$*. Then for all* $1 \leqslant i \leqslant n$*, the nonzero entries in the matrices*

$$[B^{(2)}_{i,i+1}, B^{(2)}_{i,i+2}, \ldots, B^{(2)}_{i,i+n-1}] \qquad \textit{and}$$
$$[B^{(2)}_{i+1,i}, B^{(2)}_{i+2,i}, \ldots, B^{(2)}_{i+n-1,i}]$$

Please cite this article in press as: J. Pappe et al., Promotion and growth diagrams for fans of Dyck paths and vacillating tableaux, J. Algebra (2023), https://doi.org/10.1016/j.jalgebra.2023.07.038

form a north-east chain. In particular, we have

$$\mathsf{blowup}_2^{\mathsf{NE}} \circ \mathsf{M}_{V\to O} = \mathsf{M}_O \circ \iota_{V\to O}.$$

Proof. From Propositions 3.2 and 3.13, it suffices to prove that the nonzero entries in $[B^{(2)}_{n,n+1}, B^{(2)}_{n,n+2}, \dots, B^{(2)}_{n,2n-1}]$ and $[B^{(2)}_{2,1}, B^{(2)}_{3,1}, \dots, B^{(2)}_{n,1}]^T$ form a south-east chain. Recall that by construction, the Fomin growth diagram of $\iota_{V\to O}(\mathsf{V})$ is a triangle diagram with the entries of $\iota_{V\to O}(\mathsf{V})$ labeling its diagonal. As V is a vacillating tableau of weight zero, the partition (2) sits at the corners $(2, 2(n-1))$ and $(2(n-1), 2)$ in the Fomin growth diagram of $\iota_{V\to O}(\mathsf{V})$. By Theorem 4.4, we have $\mathsf{M}_O(\iota_{V\to O}(\mathsf{V})) = \mathsf{G}_O(\iota_{V\to O}(\mathsf{V}))$. This implies that the filling of the first 2 columns and first 2 rows matches $\mathsf{M}_O(\iota_{V\to O}(\mathsf{V}))$. As all the entries of $\mathsf{M}_O(\iota_{V\to O}(\mathsf{V}))$ are either 0 or 1, we have that all the nonzero entries in the first 2 rows and the first 2 rows form a north-east chain by [21, Theorem 2]. □

We can now prove the first part of Theorem 4.11.

Proof. Putting together the current results we obtain:

$$\begin{aligned} \mathsf{blowup}_2^{\mathsf{NE}} \circ \mathsf{M}_{V\to O} &= \mathsf{M}_O \circ \iota_{V\to O} && \text{by Lemma 4.15} \\ &= \mathsf{G}_O \circ \iota_{V\to O} && \text{by Theorem 4.4.} \end{aligned}$$

It thus remains to show: $\mathsf{G}_V = \mathsf{blocksum}_2 \circ \mathsf{G}_O \circ \iota_{V\to O}$. Let V be a fixed vacillating tableau of weight zero and length n. Let $\mathsf{O} = \iota_{V\to O}(\mathsf{V})$. Let $M = (m_{i,j})_{1\leqslant i,j\leqslant 2n} = \mathsf{G}_O(\mathsf{O})$ and let $B^{(2)}_{i,j}$ be its block matrix decomposition. Let $\alpha_{i,j}$ for $0 \leqslant j \leqslant i \leqslant 2n$ be the partition in the i-th row and j-th column in the growth diagram of O. Above calculation shows that the nonzero entries in the matrices

$$[B^{(2)}_{i,i+1}, B^{(2)}_{i,i+2}, \dots, B^{(2)}_{i,i+n-1}] \qquad \text{and}$$
$$[B^{(2)}_{i+1,i}, B^{(2)}_{i+2,i}, \dots, B^{(2)}_{i+n-1,i}]$$

form north-east chains.

Thus the squares

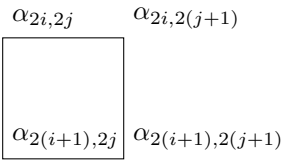

with entry $m_{2i,2j} + m_{2i+1,2j} + m_{2i,2j+1} + m_{2i+1,2j+1}$ satisfy the rules RSK F0-F2 and RSK B0-B2. As in proof of Lemma 4.14, the entries of the first subdiagonal of M are zero. Hence M is uniquely determined by the labels $\alpha 2i, 2i$ and $\alpha_{2i,2i+1}$. Again by proof

of Lemma 4.14 we have $\alpha_{2i,2i} = 2\lambda^i$ and $\alpha_{2i,2i+1} = (2\lambda^i) \cup (2\lambda^{i+1})$. As these partitions agree with the labels in Construction 3.18, we get $\mathsf{G}_V(\mathsf{V}) = \mathsf{blocksum}_2(\mathsf{G}_O(\mathsf{O}))$. □

Problem 4.16. Find a characterization of the image of the injective maps M_F, $\mathsf{M}_{V\to O}$ and $\mathsf{M}_{V\to F}$.

Remark 4.17. For M_O the solution to the above problem is known (see [30]). The set of r-symplectic oscillating tableaux of weight zero are in bijection with the set of $(r+1)$-noncrossing perfect matchings of $\{1, 2, \ldots, n\}$.

4.4. Cyclic sieving

The cyclic sieving phenomenon was introduced by Reiner, Stanton and White [33] as a generalization of Stembridge's $q = -1$ phenomenon.

Definition 4.18. Let X be a finite set and C be a cyclic group generated by c acting on X. Let $\zeta \in \mathbb{C}$ be a $|C|^{th}$ primitive root of unity and $f(q) \in \mathbb{Z}[q]$ be a polynomial in q. Then the triple (X, C, f) exhibits the *cyclic sieving phenomenon* if for all $d \geqslant 0$ we have that the size of the fixed point set of c^d (denoted X^{c^d}) satisfies $|X^{c^d}| = f(\zeta^d)$.

In this section, we will state cyclic sieving phenomena for the promotion action on oscillating tableaux, fans of Dyck paths, and vacillating tableaux. In Section 4.4.1 we review an approach using the energy function. In Sections 4.4.2 and 4.4.3 we give new cyclic sieving phenomena for fans of Dyck paths and vacillating tableaux, respectively.

4.4.1. Cyclic sieving using the energy function

We first introduce the energy function on tensor products of crystals. The energy function is defined on affine crystals, meaning that the crystal $\mathcal{C}_\square$ needs to be upgraded to a crystal of affine Kac–Moody type $C_r^{(1)}$ and the crystals $\mathcal{B}_\square$ and $\mathcal{B}_{\mathsf{spin}}$ need to be upgraded to crystals of affine Kac–Moody type $B_r^{(1)}$. In particular, these affine crystals have additional crystals operators f_0 and e_0. For further details, see for example [27,25, 10].

For an affine crystal $\mathcal{B}$, the *local energy function*

$$H : \mathcal{B} \otimes \mathcal{B} \to \mathbb{Z}$$

is defined recursively (up to an overall constant) by

$$H(e_i(b_1 \otimes b_2)) = H(b_1 \otimes b_2) + \begin{cases} +1 & \text{if } i = 0 \text{ and } \varepsilon_0(b_1) > \varphi_0(b_2), \\ -1 & \text{if } i = 0 \text{ and } \varepsilon_0(b_1) \leqslant \varphi_0(b_2), \\ 0 & \text{otherwise.} \end{cases}$$

Please cite this article in press as: J. Pappe et al., Promotion and growth diagrams for fans of Dyck paths and vacillating tableaux, J. Algebra (2023), https://doi.org/10.1016/j.jalgebra.2023.07.038

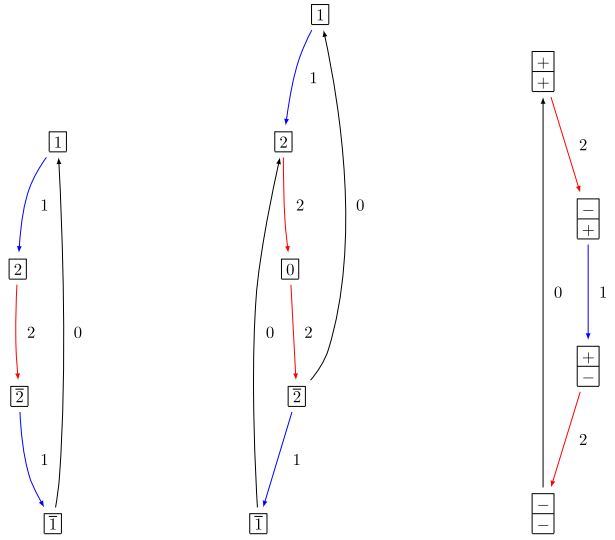

Fig. 13. Left: Affine crystal $\mathcal{C}^{\mathsf{af}}_{\square}$ of type $C^{(1)}_2$. Middle: Affine crystal $\mathcal{B}^{\mathsf{af}}_{\square}$ of type $B^{(1)}_2$. Right: Affine crystal $\mathcal{B}^{\mathsf{af}}_{\mathsf{spin}}$ of type $B^{(1)}_2$.

The crystals we consider here are simple, meaning that there exists a dominant weight λ such that $\mathcal{B}$ contains a unique element, denoted $u(\mathcal{B})$, of weight λ such that every extremal vector of $\mathcal{B}$ is contained in the Weyl group orbit of λ. We normalize H such that

$$H(u(\mathcal{B}) \otimes u(\mathcal{B})) = 0.$$

Example 4.19. The affine crystal $\mathcal{C}^{\mathsf{af}}_{\square}$ of type $C^{(1)}_r$ is, for example, constructed in [10, Theorem 5.7]. The case of type $C^{(1)}_2$ is depicted in Fig. 13. Using the ordering $1 < 2 < \cdots < r < \overline{r} < \cdots < \overline{2} < \overline{1}$, we have that $H(a \otimes b) = 0$ if $a \leqslant b$ and $H(a \otimes b) = 1$ if $a > b$.

Example 4.20. The affine crystal $\mathcal{B}^{\mathsf{af}}_{\square}$ of type $B^{(1)}_r$ is, for example, constructed in [10, Theorem 5.1]. The case $B^{(1)}_2$ is depicted in Fig. 13. Using the ordering $1 < 2 < \cdots < r < 0 < \overline{r} < \cdots < \overline{2} < \overline{1}$, we have that $H(a \otimes b) = 0$ if $a \leqslant b$ and $a \otimes b \neq 0 \otimes 0$, $H(\overline{1} \otimes 1) = 2$, and $H(a \otimes b) = 1$ otherwise.

Example 4.21. The affine crystal $\mathcal{B}^{\mathsf{af}}_{\mathsf{spin}}$ of type $B^{(1)}_r$ is constructed in [10, Theorem 5.3]. The case $B^{(1)}_2$ is depicted in Fig. 13. The classical highest weight elements in $\mathcal{B}^{\mathsf{af}}_{\mathsf{spin}} \otimes \mathcal{B}^{\mathsf{af}}_{\mathsf{spin}}$ are $(\epsilon_1, \ldots, \epsilon_r) \otimes (+, +, \ldots, +)$ with $\epsilon_i = +$ for $1 \leqslant i \leqslant k$ and $\epsilon_i = -$ for $k < i \leqslant r$ for some $0 \leqslant k \leqslant r$. Denoting by $m(\epsilon_1, \ldots, \epsilon_r)$ the number of $-$ in the ϵ_i, we have

$$H((\epsilon_1, \ldots, \epsilon_r) \otimes (+, \ldots, +)) = \left\lfloor \frac{m(\epsilon_1, \ldots, \epsilon_r) + 1}{2} \right\rfloor.$$

By definition, the local energy is constant on classical components.

Please cite this article in press as: J. Pappe et al., Promotion and growth diagrams for fans of Dyck paths and vacillating tableaux, J. Algebra (2023), https://doi.org/10.1016/j.jalgebra.2023.07.038

The *energy function*

$$E\colon \mathcal{B}^{\otimes n} \to \mathbb{Z}$$

is defined as follows for $b_1 \otimes \cdots \otimes b_n \in \mathcal{B}^{\otimes n}$

$$E(b_1 \otimes \cdots \otimes b_n) = \sum_{i=1}^{n-1} iH(b_i \otimes b_{i+1}).$$

Let us now define a polynomial in q using the energy function for highest weight elements in $\mathcal{B}^{\otimes n}$ of weight zero

$$f_{n,r}(q) = q^{c_{n,r}} \sum_{\substack{b\in\mathcal{B}^{\otimes n}\\ \mathsf{wt}(b)=0\\ e_i(b)=0 \text{ for } 1\leqslant i\leqslant r}} q^{E(b)},$$

where r is the rank of the type of the underlying root system and $c_{n,r}$ is a constant depending on the type. Namely,

$$c_{n,r} = \begin{cases} 0 & \text{for } \mathcal{B}_{\square} \text{ all } r \text{ and } \mathcal{B}_{\mathsf{spin}} \text{ for } r \equiv 0,3 \pmod 4,\\ q^{\frac{n}{2}} & \text{for } \mathcal{C}_{\square} \text{ all } r \text{ and } \mathcal{B}_{\mathsf{spin}} \text{ for } r \equiv 1,2 \pmod 4. \end{cases}$$

The following theorem clarifies statements in [43].

Theorem 4.22. *Let X be the set of highest weight elements in $\mathcal{B}^{\otimes n}$ of weight zero, where the Kirillov–Reshetikhin crystal corresponding to $\mathcal{B}$ is classically irreducible. Then $(X, C_n, f_{n,r}(q))$ exhibits the cyclic sieving phenomenon, where C_n is the cyclic group of order n on n tensor factors inherited from the evaluation modules as in [7, Theorem 4.2].*

Proof. In [7, Proof of Theorem 4.2], Fontaine and Kamnitzer proved that $(X, C_n, \widetilde{f}_{n,r}(q))$ exhibits the cyclic sieving phenomenon, where $\widetilde{f}_{n,r}(q)$ is a polynomial defined in terms of current algebra actions on Weyl modules of Fourier and Littelmann [8]. These arguments use that the fusion product is independent of the parameters, which was proven by Ardonne and Kedem [1]. When the Kirillov–Reshetikhin crystals are classically irreducible, the cyclic vectors for the evaluation representations are uniquely determined as the tensor product of classically highest weight elements. By [11], this polynomial is equal to the energy function polynomial up to an overall constant, proving the claim. □

When the crystal $\mathcal{B}$ is minuscule, it was shown by Fontaine and Kamnitzer [7] that the cyclic action on $\mathcal{B}^{\otimes n}$ is given by promotion. In particular, for oscillating tableaux and fans of Dyck paths Theorem 4.22 gives a cyclic sieving phenomenon with the promotion

Please cite this article in press as: J. Pappe et al., Promotion and growth diagrams for fans of Dyck paths and vacillating tableaux, J. Algebra (2023), https://doi.org/10.1016/j.jalgebra.2023.07.038

action since the corresponding crystals are minuscule. The crystals corresponding to vacillating tableaux are not minuscule.

For the vector representation of type A, highest weight elements in the tensor product of weight zero under RSK are in correspondence with standard tableaux of rectangular shape. The energy function relates to the major index under correspondence. Hence in this case, Theorem 4.22 relates to results in [31].

Note that the Kirillov–Reshetikhin crystals corresponding to $\mathcal{C}_{\square}$, $\mathcal{B}_{\mathsf{spin}}$, and $\mathcal{B}_{\square}$ are classically irreducible, and hence Theorem 4.22 gives a cyclic sieving phenomenon for oscillating tableaux, fans of Dyck paths, and vacillating tableaux.

4.4.2. Cyclic sieving for fans of Dyck paths

Recall from Section 2.3.2 that highest weight elements of weight zero in $\mathcal{B}_{\mathsf{spin}}^{\otimes 2n}$ of type B_r are in bijection with r-fans of Dyck paths of length $2n$. Denote by $D_n^{(r)}$ the set of all r-fans of Dyck paths of length $2n$. The cardinality of this set is given by $\prod_{1\leqslant i\leqslant j\leqslant n-1} \frac{i+j+2r}{i+j}$, see [6,20]. Define the q-analogue of this formula as

$$g_{n,r}(q) = \prod_{1\leqslant i\leqslant j\leqslant n-1} \frac{[i+j+2r]_q}{[i+j]_q}, \tag{4.3}$$

where $[m]_q = 1 + q + q^2 + \cdots + q^{m-1}$.

Conjecture 4.23. *The triple $(D_n^{(r)}, C_{2n}, g_{n,r}(q))$ exhibits the cyclic sieving phenomenon, where C_{2n} is the cyclic group of order $2n$ that acts on $D_n^{(r)}$ by applying promotion.*

Example 4.24. We have

$$q^{-4} f_{4,2}(q) = g_{2,2}(q) = q^4 + q^2 + 1$$

and

$$\begin{aligned} g_{3,2}(q) &= q^{12} + q^{10} + q^9 + 2q^8 + q^7 + 2q^6 + q^5 + 2q^4 + q^3 + q^2 + 1, \\ q^{-6} f_{6,2}(q) &= q^{10} + q^9 + 2q^8 + q^7 + 3q^6 + q^5 + 2q^4 + q^3 + q^2 + 1. \end{aligned}$$

Note that $g_{3,2}(q) = f_{6,2}(q) \pmod{q^6 - 1}$.

In general, we conjecture that $g_{n,r}(q) = f_{2n,r}(q) \pmod{q^{2n}-1}$ which has been verified for all $n + r \leqslant 10$.

Note that by [20, Theorem 10]

$$g_{n,r}(q) = \prod_{1\leqslant i\leqslant j\leqslant n-1} \frac{[i+j+2r]_q}{[i+j]_q} = \sum_{\substack{\lambda \\ \lambda_1 \leqslant r}} s_{2\lambda}(q, q^2, \ldots, q^{n-1}).$$

Please cite this article in press as: J. Pappe et al., Promotion and growth diagrams for fans of Dyck paths and vacillating tableaux, J. Algebra (2023), https://doi.org/10.1016/j.jalgebra.2023.07.038

Remark 4.25. Conjecture 4.23 is equivalent to [13, Conjecture 5.2], [15, Conjecture 4.28], and [14, Conjecture 5.9] on plane partitions and root posets.

Remark 4.26. There is a bijection between r-fans of Dyck paths of length $2(n-2r)$ and r-triangulations of n-gons. A cyclic sieving phenomenon in this setting was conjectured by Serrano and Stump [36]. Even though the polynomial in this conjectured cyclic sieving phenomenon is $g_{n-2r,r}$, the cyclic group acting is C_{2n}, which is different from our setting.

4.4.3. Cyclic sieving for vacillating tableaux

Before giving our cyclic sieving phenomenon result for vacillating tableaux, we review Jagenteufel's major statistic for vacillating tableaux [16]. As vacillating tableaux are in bijection with highest weight elements of $\mathcal{B}_{\square}^{\otimes n}$, it suffices to define the major statistic on highest weight elements of $\mathcal{B}_{\square}^{\otimes n}$.

Let $u = u_n \otimes \cdots \otimes u_2 \otimes u_1$ be a highest weight element in $\mathcal{B}_{\square}^{\otimes n}$ of type B_r. As before let $<$ denote the ordering $1 < 2 < \cdots < r < 0 < \bar{r} < \cdots < \bar{2} < \bar{1}$ on the elements of $\mathcal{B}_{\square}$. We say that position i is a *descent* for u if

(1) $u_{i+1} > u_i$, and
(2) if the suffix $u_{i-1} \otimes \cdots \otimes u_2 \otimes u_1$ has an equal number of j's and $\bar{j}$'s, then $u_{i+1} \otimes u_i \neq \bar{j} \otimes j$.

Denote the set of descents of u by $\mathsf{Des}(u)$. Define the *major index* of u, denoted by $\mathrm{maj}(u)$, as the sum of its descents $\sum_{i \in \mathsf{Des}(u)} i$. Let $h_{n,r}(q)$ denote the polynomial in q given by

$$h_{n,r}(q) = \sum_{u \in V_n^{(r)}} q^{\mathrm{maj}(u)}$$

where $V_n^{(r)}$ denotes the set of all highest weight elements of weight zero in $\mathcal{B}_{\square}^{\otimes n}$ of type B_r.

From [16, Theorem 2.1] and [43, Theorem 6.8], we obtain the following result.

Theorem 4.27. *The triple $(V_n^{(r)}, C_n, h_{n,r}(q))$ exhibits the cyclic sieving phenomenon, where the cyclic group on n elements, C_n, acts on $V_n^{(r)}$ by applying promotion.*

Using the descent-preserving bijection in [16], we obtain another interpretation of $h_{n,r}(q)$ in terms of standard Young tableaux. Adopting the notation and terminology of [37] for standard Young tableaux, we say that i is a descent for the standard Young tableau T if $i+1$ sits in a lower row than i in T in English notation. Given this, we analogously define $\mathrm{maj}(T)$ to be the sum of the descents of T. Letting $\mathrm{SYT}(\lambda)$ denote the set of all standard Young tableaux of shape λ, the polynomial $h_{n,r}(q)$ can be reinterpreted as follows.

Please cite this article in press as: J. Pappe et al., Promotion and growth diagrams for fans of Dyck paths and vacillating tableaux, J. Algebra (2023), https://doi.org/10.1016/j.jalgebra.2023.07.038

Theorem 4.28. *[16] Let $n, r \geqslant 1$. Then*

$$h_{n,r}(q) = \sum_{T \in \mathrm{SYT}(\lambda)} q^{\mathrm{maj}(T)},$$

where λ ranges over all partitions of n with only even parts and length at most $2r+1$ when n is even and λ ranges over all partitions of n with only odd parts and length exactly $2r+1$ when n is odd.

Example 4.29. We have

$$f_{7,2}(q) = q^{22} + q^{21} + q^{20} + q^{19} + 2q^{18} + 2q^{17} + 2q^{16} + q^{15} + 2q^{14} + q^{13} + q^{12}$$
$$h_{7,2}(q) = q^{18} + q^{17} + 2q^{16} + 2q^{15} + 3q^{14} + 2q^{13} + 2q^{12} + q^{11} + q^{10}$$

Note that $f_{7,2}(q) = h_{7,2}(q) \pmod{q^7 - 1}$.

Data availability

No data was used for the research described in the article.

References

[1] Eddy Ardonne, Rinat Kedem, Fusion products of Kirillov-Reshetikhin modules and fermionic multiplicity formulas, J. Algebra 308 (1) (2007) 270–294. MR 2290922.
[2] Arvind Ayyer, Steven Klee, Anne Schilling, Combinatorial Markov chains on linear extensions, J. Algebraic Comb. 39 (4) (2014) 853–881. MR 3199029.
[3] Daniel Bump, Anne Schilling, Crystal Bases. Representations and Combinatorics, World Scientific Publishing Co. Pte. Ltd., Hackensack, NJ, 2017. MR 3642318.
[4] Jason Bandlow, Anne Schilling, Nicolas M. Thiéry, On the uniqueness of promotion operators on tensor products of type A crystals, J. Algebraic Comb. 31 (2) (2010) 217–251. MR 2592077.
[5] Sabin Cautis, Joel Kamnitzer, Scott Morrison, Webs and quantum skew Howe duality, Math. Ann. 360 (1–2) (2014) 351–390. MR 3263166.
[6] Myriam de Sainte-Catherine, Gérard Viennot, Enumeration of certain Young tableaux with bounded height, in: Combinatoire énumérative, Montreal, Que., 1985/Quebec, Que., 1985, in: Lecture Notes in Math., vol. 1234, Springer, Berlin, 1986, pp. 58–67. MR 927758.
[7] Bruce Fontaine, Joel Kamnitzer, Cyclic sieving, rotation, and geometric representation theory, Sel. Math. New Ser. 20 (2) (2014) 609–625. MR 3177928.
[8] G. Fourier, P. Littelmann, Weyl modules, Demazure modules, KR-modules, crystals, fusion products and limit constructions, Adv. Math. 211 (2) (2007) 566–593. MR 2323538.
[9] S.V. Fomin, The generalized Robinson-Schensted-Knuth correspondence, in: Differentsial'naya Geometriya, Gruppy Li i Mekh. VIII, Zap. Nauchn. Sem. Leningrad. Otdel. Mat. Inst. Steklov. (LOMI) 155 (1986) 156–175, 195, translation in J. Sov. Math. 41 (2) (1988) 979–991. MR 869582.
[10] Ghislain Fourier, Masato Okado, Anne Schilling, Kirillov-Reshetikhin crystals for nonexceptional types, Adv. Math. 222 (3) (2009) 1080–1116. MR 2553378.
[11] Ghislain Fourier, Anne Schilling, Mark Shimozono, Demazure structure inside Kirillov-Reshetikhin crystals, J. Algebra 309 (1) (2007) 386–404. MR 2301245.
[12] André Henriques, Joel Kamnitzer, Crystals and coboundary categories, Duke Math. J. 132 (2) (2006) 191–216. MR 2219257.
[13] Sam Hopkins, Cyclic sieving for plane partitions and symmetry, SIGMA 16 (2020) 130. MR 4184618.
[14] Sam Hopkins, Order polynomial product formulas and poset dynamics, preprint arXiv:2006.01568, 2020.

Please cite this article in press as: J. Pappe et al., Promotion and growth diagrams for fans of Dyck paths and vacillating tableaux, J. Algebra (2023), https://doi.org/10.1016/j.jalgebra.2023.07.038

[15] Sam Hopkins, Minuscule doppelgängers, the coincidental down-degree expectations property, and rowmotion, Exp. Math. 31 (3) (2022) 946–974. MR 4477416.
[16] Judith Jagenteufel, A Sundaram type bijection for SO($2k+1$): vacillating tableaux and pairs consisting of a standard Young tableau and an orthogonal Littlewood-Richardson tableau, Sémin. Lothar. Comb. 82B (2020) 33. MR 4098254.
[17] Masaki Kashiwara, Crystalizing the q-analogue of universal enveloping algebras, Commun. Math. Phys. 133 (2) (1990) 249–260. MR 1090425.
[18] Masaki Kashiwara, Similarity of crystal bases, in: Lie Algebras and Their Representations, Seoul, 1995, in: Contemp. Math., vol. 194, Amer. Math. Soc., Providence, RI, 1996, pp. 177–186. MR 1395599.
[19] Mikhail Khovanov, Greg Kuperberg, Web bases for sl(3) are not dual canonical, Pac. J. Math. 188 (1) (1999) 129–153. MR 1680395.
[20] C. Krattenthaler, The major counting of nonintersecting lattice paths and generating functions for tableaux, Mem. Am. Math. Soc. 115 (552) (1995). MR 1254150.
[21] C. Krattenthaler, Growth diagrams, and increasing and decreasing chains in fillings of Ferrers shapes, Adv. Appl. Math. 37 (3) (2006) 404–431. MR 2261181.
[22] Greg Kuperberg, Spiders for rank 2 Lie algebras, Commun. Math. Phys. 180 (1) (1996) 109–151. MR 1403861.
[23] Cristian Lenart, On the combinatorics of crystal graphs. II. The crystal commutor, Proc. Am. Math. Soc. 136 (3) (2008) 825–837. MR 2361854.
[24] G. Lusztig, Canonical bases arising from quantized enveloping algebras, J. Am. Math. Soc. 3 (2) (1990) 447–498. MR 1035415.
[25] Masato Okado, Anne Schilling, Existence of Kirillov-Reshetikhin crystals for nonexceptional types, Represent. Theory 12 (2008) 186–207. MR 2403558.
[26] Se-jin Oh, Travis Scrimshaw, Identities from representation theory, Discrete Math. 342 (9) (2019) 2493–2541. MR 3959676.
[27] Masato Okado, Anne Schilling, Mark Shimozono, Virtual crystals and fermionic formulas of type $D_{n+1}^{(2)}$, $A_{2n}^{(2)}$, and $C_n^{(1)}$, Represent. Theory 7 (2003) 101–163. MR 1973369.
[28] Rebecca Patrias, Promotion on generalized oscillating tableaux and web rotation, J. Comb. Theory, Ser. A 161 (2019) 1–28. MR 3861768.
[29] T. Kyle Petersen, Pavlo Pylyavskyy, Brendon Rhoades, Promotion and cyclic sieving via webs, J. Algebraic Comb. 30 (1) (2009) 19–41. MR 2519848.
[30] Stephan Pfannerer, Martin Rubey, Bruce Westbury, Promotion on oscillating and alternating tableaux and rotation of matchings and permutations, Algebraic Combin. 3 (1) (2020) 107–141. MR 4068745.
[31] Brendon Rhoades, Cyclic sieving, promotion, and representation theory, J. Comb. Theory, Ser. A 117 (1) (2010) 38–76. MR 2557880.
[32] Thomas Walton V. Roby, Applications and extensions of Fomin's generalization of the Robinson-Schensted correspondence to differential posets, ProQuest LLC, Ann Arbor, MI, 1991, Thesis (Ph.D.)–Massachusetts Institute of Technology. MR 2716353.
[33] V. Reiner, D. Stanton, D. White, The cyclic sieving phenomenon, J. Comb. Theory, Ser. A 108 (1) (2004) 17–50.
[34] G. Rumer, E. Teller, H. Weyl, Eine für die Valenztheorie geeignete Basis der binären Vektorinvarianten, Nachr. Ges. Wiss. Gött., Math.-Phys. Kl. 1932 (1932) 499–504.
[35] Heather M. Russell, An explicit bijection between semistandard tableaux and non-elliptic sl_3 webs, J. Algebraic Comb. 38 (4) (2013) 851–862. MR 3119361.
[36] Luis Serrano, Christian Stump, Maximal fillings of moon polyominoes, simplicial complexes, and Schubert polynomials, Electron. J. Comb. 19 (1) (2012) 16. MR 2880647.
[37] Richard P. Stanley, Enumerative Combinatorics, vol. 2, Cambridge Studies in Advanced Mathematics, vol. 62, Cambridge University Press, Cambridge, 1999. With a foreword by Gian-Carlo Rota and appendix 1 by Sergey Fomin. MR 1676282.
[38] Richard P. Stanley, Promotion and evacuation, in: Special volume in honor of Anders Björner, Electron. J. Comb. 16 (2) (2009). Research Paper 9, 24. MR 2515772.
[39] John R. Stembridge, A local characterization of simply-laced crystals, Trans. Am. Math. Soc. 355 (12) (2003) 4807–4823. MR 1997585.
[40] Sheila Sundaram, Orthogonal tableaux and an insertion algorithm for SO($2n+1$), J. Comb. Theory, Ser. A 53 (2) (1990) 239–256. MR 1041447.
[41] Marc A.A. van Leeuwen, An analogue of jeu de taquin for Littelmann's crystal paths, Sémin. Lothar. Comb. 41 (1998) B41b. MR 1661263.

Please cite this article in press as: J. Pappe et al., Promotion and growth diagrams for fans of Dyck paths and vacillating tableaux, J. Algebra (2023), https://doi.org/10.1016/j.jalgebra.2023.07.038

[42] Marc A.A. van Leeuwen, Spin-preserving Knuth correspondences for ribbon tableaux, Electron. J. Comb. 12 (2005). Research Paper 10, 65. MR 2134173.
[43] Bruce W. Westbury, Invariant tensors and the cyclic sieving phenomenon, Electron. J. Comb. 23 (4) (2016) 4.25. MR 3577672.
[44] Bruce W. Westbury, Coboundary categories and local rules, Electron. J. Comb. 25 (4) (2018) 4.9. MR 3874275.

Please cite this article in press as: J. Pappe et al., Promotion and growth diagrams for fans of Dyck paths and vacillating tableaux, J. Algebra (2023), https://doi.org/10.1016/j.jalgebra.2023.07.038